AD-787 741

GLASSY CARBON, ALLOYS

PENNSYLVANIA STATE UNIVERSITY

PREPARED FOR

ADVANCED RESEARCH PROJECTS AGENCY

15 OCTOBER 1974

DISTRIBUTED BY:

NTIS
National Technical Information Service
U. S. DEPARTMENT OF COMMERCE

AD 787741

FINAL REPORT

GLASSY CARBON, ALLOYS

Sponsored By

Advanced Research Projects Agency
Arlington, Virginia

October 15, 1974

P. L. Walker, Jr.
(814) 865-0497

The Pennsylvania State University

Department of Material Sciences

and the

Materials Research Laboratory

University Park, Pennsylvania 16802

Contract Amount: $259,019 Contract Period: June 1, 1971-May 31, 1974

TABLE OF CONTENTS

FINAL REPORT

October 15, 1974

GLASSY CARBON, ALLOYS

SUMMARY

Glassy carbons show promise of having a wide use in defense and space applications -- as well as a number of civilian-oriented spin-offs. Artifacts can be made in large shapes. Glassy carbons have a range of properties which are of interest such as impermeability to gases, despite the fact that they have significant porosity. Obviously the porosity is closed. As a result of low permeability, the oxidation rate of glassy carbon is low. As a result of a low oxidation rate and the ability to produce artifacts in a single phase (rather than a composite), the ablation performance of glassy carbon, particularly at high pressures, is excellent. The considerable porosity in glassy carbons results in their having a reasonably low coefficient of thermal expansion and, hence, reasonably good thermal shock resistance. Again this is important in defense and space applications where materials undergo large, sudden changes in temperature.

In the case of inorganic glasses, it has been common to modify and improve their properties by the addition of other elements. For vapor deposited carbons, it is not uncommon to incorporate one or more additional elements to improve some property such as fracture strength -- for example, silicon addition to isotropic carbons. It is almost inconceivable that the desired properties of glassy carbons have been optimized chemically at the pure element composition. Therefore, this research program has had as one of its <u>main objectives to determine the</u>

possibilities of ultimately modifying the structure and properties of glassy carbon by the addition of various elements to the starting organic precursors.

This laboratory has shown recently that the use of elevated pressure during carbonization of organic precursors is a powerful variable to yield both low and high temperature carbons of widely different structures and properties. Other workers have shown that polymerization of organic precursors under pressure (prior to their carbonization) can lead to polymers of variable and interesting morphology. Hence, another main objective of this research program has been to study the effects of the application of pressure during polymerization and/or carbonization of glassy carbon precursors on the structure and properties of carbons produced.

During the course of this research program, several other approaches at producing glassy or disordered carbons have also been explored. They are: i) production of carbon composites by the infiltration of porous carbon artifacts with pyrolytic carbon and ii) production of films of binary mixtures of disordered carbon and carbide by sputtering. Progress and major results achieved in each area in which we had activities will now be summarized in this final report.

I. Glassy Carbons as Modified by Addition of Metals

The organic precursor which was used in much of the program to produce glassy carbons was furfuryl alcohol, which is reasonably cheap and has a high coking value. An in-depth study was conducted on the possibilities of modifying the properties of the glassy carbon made from furfuryl alcohol by the addition of iron-containing organic compounds into the original "mix". Results of this study are presented in published form in CARBON, 12, 281-289 (1974). In summary, glassy carbons containing iron were prepared from copolymers of furfuryl alcohol and ferrocene derivatives at heat-treatment temperatures from 500°C to 2500°C. The copolymerization produced a highly dispersed state of iron in carbonaceous matrices at least in the early stage of pyrolysis. Above 500°C, the homogeneously dispersed iron separated into irregularly spaced domains consisting of cementite, pure iron and iron compounds of unknown composition. Addition of iron resulted in a local graphitization of the glassy carbon at heat-treatment temperatures above 1000°C. At heat-treatment temperatures between 500°C and 800°C, electrical resistivities of the iron-doped carbons were much smaller than those of unmodified polyfurfuryl alcohol carbons but followed more or less the behavior of the latter for heat-treatment temperatures above 800°C. Measurements of mechanical properties indicated a remarkable increase in tensile strength of the low temperature carbons (500°C) with increasing iron content but the strength of the iron containing carbons decreased at higher carbonization temperatures.

Another approach taken at producing metal-modified glassy carbons has been to prepare composites consisting of carbon filler from furfuryl alcohol, boron powder, and binder polymer. Progress in this area is discussed at length in this report. It is shown that samples can be prepared which have significantly greater abrasion resistance and hardness than steel and commercially available glassy carbon. In addition, the processing time is less than that required for conventional glassy carbons.

We conclude that there is excellent potential for applications of glassy and disordered carbons modified by addition of metals. Our studies have, in our judgment, just "scratched the surface" as to the possibilities in this area.

II. Glassy Carbons Produced by Processing Precursors Under High Pressure

This portion of the research program was designed to meet double objectives, one of them muted (but nevertheless important), and the latter was that the results should lead readily to the making of pieces of massive compact glassy carbon that would be adequate for conventional electrical and mechanical testing. The open objective was to modify the precursors during polymerization and carbonization under pressure so as to produce glassy carbons with significantly altered properties.

It was found that the precursors were responsive to the pressure variable, and that carbons were obtained generally in accord with expectations. The results are reported in the semi-annual reports and letters covering the project. They shall be summarized in this manner:

a) The initial experiences with pressure-temperature processing over the range to 3 kbar and 900°C soon restricted the starting materials to divinylbenzene (DVB) and furfuryl alcohol (FA). The particulate and vesiculated carbons obtained did not warrant exploratory use of related materials.

b) Selected organo-metallics, added with the idea of building into the polymer a homogeneously dispersed metallic atom or a potential carbon "cage", could be incorporated in amounts of a few percent. Their use did lead to carbons of different morphologies and properties on heating the polymers to 500-2000°C.

c) Pressure definitely accelerated polymerization to the point that no catalysts were necessary for DVB. Density, viscosity, refractive indices were affected positively by pressure. The influence of these differences was blurred at the higher temperatures of carbonization.

d) Carbonization under pressure did produce varied and unusual results. From polymerized DVB it was possible to obtain glassy carbon as vesiculated, spherulitic or interconnected solid lacework forms with increasing pressure. The spherulitic form was of special interest because it provided important insights to the "mesophase" graphitic carbons although it was itself a glassy carbon, and as such it represented an entirely new form of carbon. Pressure carbonization of PFA generally produced randomly vesiculated carbons with poor reproducibility of strength, shape or size. However, it was noted that cast pieces of PFA could be carbonized successfully (although with internal vesiculation) at rapid heating rates while under high inert gas pressures. Considering the demanding, slow heating schedules necessary for preparing glassy carbons, there may be some profit in investigating the use of an inert gas pressure atmosphere at some stage of the heating cycle.

e) The carbonization of PDVB in permeable or impermeable (to hydrogen) noble metal tubes demonstrated the influence on the forms of carbon produced that was exerted by the composition and partial pressures of gases over a carbonizing system.

f) Various lines of experiments revealed that pressure carbonization of PDVB could produce several interesting forms of glassy carbon, those mentioned in (d) above plus permeable and impermeable glassy foams containing uniform pore sizes. However, the use of DVB was unrealistic and the <u>p-t</u> conditions impractical for larger scale production. Some effort was directed toward utilizing more common, abundant polymers mixed with solvents, tars or pitches, along with carbonization at progressively lower pressures. The major thrust was to achieve a system that would generate two immiscible liquid phases during the early stages of carbonization while under 1-20 bars pressure. Success was limited to a few runs

yielding a partly spherulitic carbon at pressures of the order of 150-250 bars.

It is concluded that the use of pressure during carbonization works against the production of glassy carbon in massive form (rods, plates), because it inhibits the diffusion of volatile products away from the polymerizing carbon mass. It did result in the production of several new forms of vesiculated, spherulitic or "spongy" glassy carbons that in themselves could serve as desirable goals if less complicated procedures were available. To take as an example, the spherulitic, glassy carbon: This material was made within a narrow range of sizes within the span of 1-10 microns. The spheres were practically without microscopically visible pores. The spheres were denser than commercial glassy carbon and very hard and strong; before shattering they would dent polished tungsten carbide surfaces. If available in bulk quantities, they could be formulated into bodies of uniform porosity and permeability, and with isotropic electrical and mechanical properties. With the control of process variables, the microporosity and micropermeability of the glass spheres themselves might be regulated, and thereby contribute to a new series of carbon bodies possessing a wide range of useful properties.

In order to realize such materials, it appears worthwhile to search for glassy carbon precursors which could be carbonized in a moderately low pressure-distillation system having provisions for controlling the composition of the vapor and liquid phases. Through this means, hopefully, a phase of two immiscible liquids could be maintained at a certain stage of carbonization, and from this point many forms of glassy carbon could then be prepared.

III. Cellulose Carbon-CVD Composites

From a number of studies it has been shown that cellulose is an excellent precursor for the production of disordered carbons. In this research cellulose powder of micron size was compacted into an artifact at 3000 psi, followed by curing and heat treatment up to 800°C. Because cellulose has a low coking value (about 19%), the structure produced is quite open and of low density. It is ideal as a substrate for the subsequent deposition of carbon from the cracking of a hydrocarbon.

In this report, there is a detailed description of the production of cellulose carbon-CVD composites using propylene as the source of CVD carbon. Composites can be produced which have superior oxidation resistance and flexural strength and lower coefficients of thermal expansion than those found in selected commercial glassy carbons. The processing of these composites is expected to be more rapid than that for glassy carbons taken to the same final temperature.

IV. Binary Glassy Carbons by Vapor Deposition Methods

One of the principal goals of this contract was the exploration of the possibility of making glassy carbons containing several percent of various other elements dispersed on an essentially atomic scale. Several approaches to this problem have been reported in our earlier reports. Among these was the approach of incorporating the various heavy metals and other elements by a method which involved vapor techniques, specifically RF sputtering. That program has proved to be very successful, and we can summarize the results as follows:

a) It is possible to prepare "glassy-carbon", or at least non-crystalline pure carbon films by sputtering.

b) Such pure carbon films can range in density from 0.5 to 1.8, the latter being the highest density attained for any form of glassy or amorphous carbon.

c) The non-crystalline or glassy carbon films can be made to incorporate from 1 to approximately 50 atom percent of virtually any heavy metal (Fe, Pt, Au, etc.). Such doped 'glassy' carbons are non-crystalline to x-ray and electron diffraction and homogeneous down to at least the 20A level.

d) In addition glassy films continuously variable in composition to 100% Ge, Si, and B can be prepared easily.

e) Such films as now developed were not too useful for corrosion prevention, since the dense phases did not adhere well to glass or steel whereas the less dense films proved to be too easily permeable.

The details on the first four items above are presented in Sections 3 and 4 of this report.

FINAL REPORT

October 15, 1974

GLASSY CARBON, ALLOYS

INTRODUCTION

Studies have been completed in four areas during the last period of this contract. In this report research results and conclusions in these following areas are considered:

1. Structural and Compositional Modification of Glassy Carbons
2. Cellulose Carbon-CVD Composites
3. New Binary Carbide "Glasses"
4. Preparation and Properties of Sputtered "Glassy Carbon Films

1. STRUCTURAL AND COMPOSITIONAL MODIFICATION OF GLASSY CARBONS

(R. Kammereck and T. Sasa)

1.1 Introduction

In recent years a number of studies have been published on the preparation and properties of composites of carbon with foreign materials such as metals or carbides. Pyrometallurgical techniques such as hot-pressing (1,2) or hot-working (3,4) in the temperature range of 2000 to 3000°C have been applied to the preparation of graphite composites with various refractory carbides. Excellent bondings of the two phases and improvements of mechanical properties were observed when the liquid phase sintering proceeded. Combination of small graphite bodies with metals or carbides into large artifacts were reported by several workers (5-9). Formation of carbide dispersions in carbon bodies utilizing a technique of initial addition of metal compounds in the carbon precursor were reported (10). Liquid metal impregnations to improve the generally porous structure of carbonaceous materials have been studied by several workers (11-14). One of the most successful examples of this technique is a highly wear resistant carbon-aluminum composite utilized as a rotary engine apex seal, which was produced by the impregnation of molten aluminum alloy in porous hard carbon bodies (15). The modifications of pyrolytic graphite with the additions of foreign elements such as boron (16) or silicon (17,18) have been studied with a codeposition technique. Studies on modifications of glassy carbon with foreign elements are very limited. Kawamura and coworkers (19) prepared glassy carbons containing metal powders of aluminum, nickel and copper. Kammereck and coworkers (20) and Yajima and coworkers (21) prepared glassy carbon containing homogeneously dispersed iron by copolymerization,

Although glassy carbon possesses highly desirable mechanical and chemical properties, the employment of this material is severely limited by the attainable dimensions of the artifacts. The problem arises in part from the evolution of pyrolysis gases during heat-treatment of polymeric precursors of glassy carbon. At pyrolysis temperatures above 350°C the organic polymer is converted into a high modulus gel which possesses among other characteristics an extremely high diffusional barrier toward evolving pyrolysis gases. In order to avoid destruction of artifacts during heat-treatment, exceedingly low heating rates have to be employed. But even at rates of 0.5°C/hour, the smallest dimension of a given sample must not exceed approximately 2 mm.

Our efforts therefore aimed not only at the improvement of glassy carbon artifacts through the addition of foreign elements but also at the development of techniques which would allow the production of artifacts of larger dimensions and at higher heating rates than are feasible with conventional methods.

1.2 Experimental

1.2.1 Preparation of materials

Glassy carbon filler was prepared from pyrolyzed polyfurfuryl alcohol, heat-treated to 1600°C in an inert atmosphere and pulverized by ball milling. The particle size ranged from 1 to 20 microns.

Boron powder, 0.5 to 5 microns in particle size, obtained from Alfa Products Ventron Corporation, was used as received.

Polytruxene, employed as binder material, was prepared by the thermal polymerization of truxene (10, 15-dihydro-5H-diindeno [1, 2-a; 1', 2'-c] fluorene), (Aldrich Chemical Company), in a nitrogen atmosphere at various temperatures above the melting point (≈320°C).

Composites were prepared by mixing appropriate quantities of carbon filler, boron and the binder polymer in an agate mortar. At times the monomer of binder material was mixed directly with the filler and polymerized together with the other ingredients. A steel die was used to produce a cylindrical pellet from the sample powder. The die was sandwiched between two plates of thermal insulation and the sidewalls of the die were enclosed in a cylindrical heating mantel. Pressure was applied on the die by a hydraulic press (Pasadena Hydraulics, Inc.). The hot-pressing was done at 430°C and 25,000 psi with a heating rate of 400°C per hour. The pellets produced were 1/2 inch in diameter and about 1/4 inch in thickness.

These pellets were then heat-treated at atmospheric pressure to 1000°C at a heating rate of 100°C per hour, and then up to 1500°C at a heating rate of 300°C per hour, and held at that temperature for 2 hours to facilitate the formation of boron carbide.

1.2.2 Measurements

Densities and porosities were either calculated directly from the geometry of the specimens or determined by mercury immersion porosimetry (American Instrument Company).

Reaction products after heat-treatment at 1500°C were examined by means of X-ray diffractometry with CuKα radiation.

Abrasive wear resistances of the specimens against SiC abrasive paper were measured as follows. SiC abrasive paper No. 320 (Buehler Ltd.) affixed on a brass disk was rotated at 180 r.p.m. in flowing water. The specimen was fixed at a position 1 inch from the center of the disk and a load of 740 g was applied on the specimen. The specimen was abraded until it showed a significant weight loss. The weight change was measured to 0.1 mg at every

500 revolutions, and at the same time the abrasive paper was renewed. The data of the abrasive wear resistance are expressed as the time required to abrade 10μ in thickness of each specimen.

Knoop microhardnesses were measured under a load of 300 g by a Miniload Hardness Tester (Ernst Leitz GMBH Wetzler) after the surfaces were polished against 0.3μ alumina slurry by means of a Vibromet Polisher (Buehler Ltd.).

The abrasive wear resistances and the hardnesses of the following five reference specimens were also measured in order to compare the data with those of the present specimens; stainless steel (Fe-18Ni-13Cr-2Mo), tool steel (Fe-1.05C-0.2Mn-0.2Si), hot-pressed corundum, glassy carbon GC-30 by Tokai Electrode Mfg. Co., and the carbon-aluminum alloy composite of the rotary engine apex seal by Nippon Carbon Company.

The microstructures of the polished surfaces of the specimens were investigated by a Stereoscan 600 Scanning Electron Microscope (Cambridge Scientific Instruments, Ltd.).

1.3 Results and Discussion

1.3.1 Preparation conditions and densities of composites

Yellow crystals of truxene transformed into a brown liquid above the melting point and then turned into a brownish, viscoelastic solid by prolonged heat-treatment. During the thermal polymerization, a substantial amount of monomer was observed to evaporate. Heat-treatment of the polymer from 440°C to 1500°C gave a glass-like hard carbon accompanied by a negligible weight loss. The polymers of truxene gave excellent compacts with glassy carbon filler by the hot-press method.

Table 1 shows formation conditions of hot-pressed specimens bound by polytruxene obtained at different polymerization temperatures. It is found

TABLE 1

HOT-PRESSED GLASSY CARBON-BORON COMPOSITES UNDER DIFFERENT PREPARATION CONDITIONS

	Initial Composition			Density (g/cc)			
Specimen Number	Boron (w/o)	Polymer (w/o)	Polymerization Condition	After Hot Press	After H.T. at 1500°C	Weight loss by H.T. (%)	Porosity After H.T. (%)
C-13	0	20	350°C 18hr[a]	1.25[c]	1.22[c]	4.3	15.6
C-14	0	20	440°C 3hr[a]	1.26[c]	1.24[c]	3.3	8.0
C-B-22	10	20	350°C 18hr[a]	1.32[c]	1.26[c]	9.1	19.1
C-B-26	35	30	440°C 1hr[b]	1.64[d]	1.61[d]	4.4	12.3
C-B-27	29	42	440°C 1hr[b]	1.57[d]	1.52[d]	6.8	15.9
C-B-29	37	26	460°C 1.5hr[b]	-	1.60[d]	5.7	8.8

a. The binder was polymerized before the mixing with the filler.
b. The binder monomer was mixed with the filler before the polymerization.
c. Apparent density calculated from geometry.
d. Density measured by mercury-immersion.

that the higher the polymerization temperature of the binder, the higher the density of the specimen obtained by the hot-press method as long as the binder retains thermoplasticity. Binders with low degree of polymerization, i.e., with low viscosity, were likely to flow out of the die during hot-pressing. The optimum polymerization temperature lies in the range from 440°C to 525°C. Heat-treatment up to 1500°C after hot-pressing resulted in a slight decrease in weight and density of the specimens.

Figure 1 shows distribution curves of pore size in a specimen (C-B-27) after hot-pressing and after heat-treatment to 1500°C. The pore size shows a sharp distribution around 0.1μ. The total porosity in the size range from 10μ to 0.01μ is observed to increase slightly with heat-treatment, while there is little change in the average pore size. More importantly, the results indicate that the pore system is formed during the hot-pressing stage,

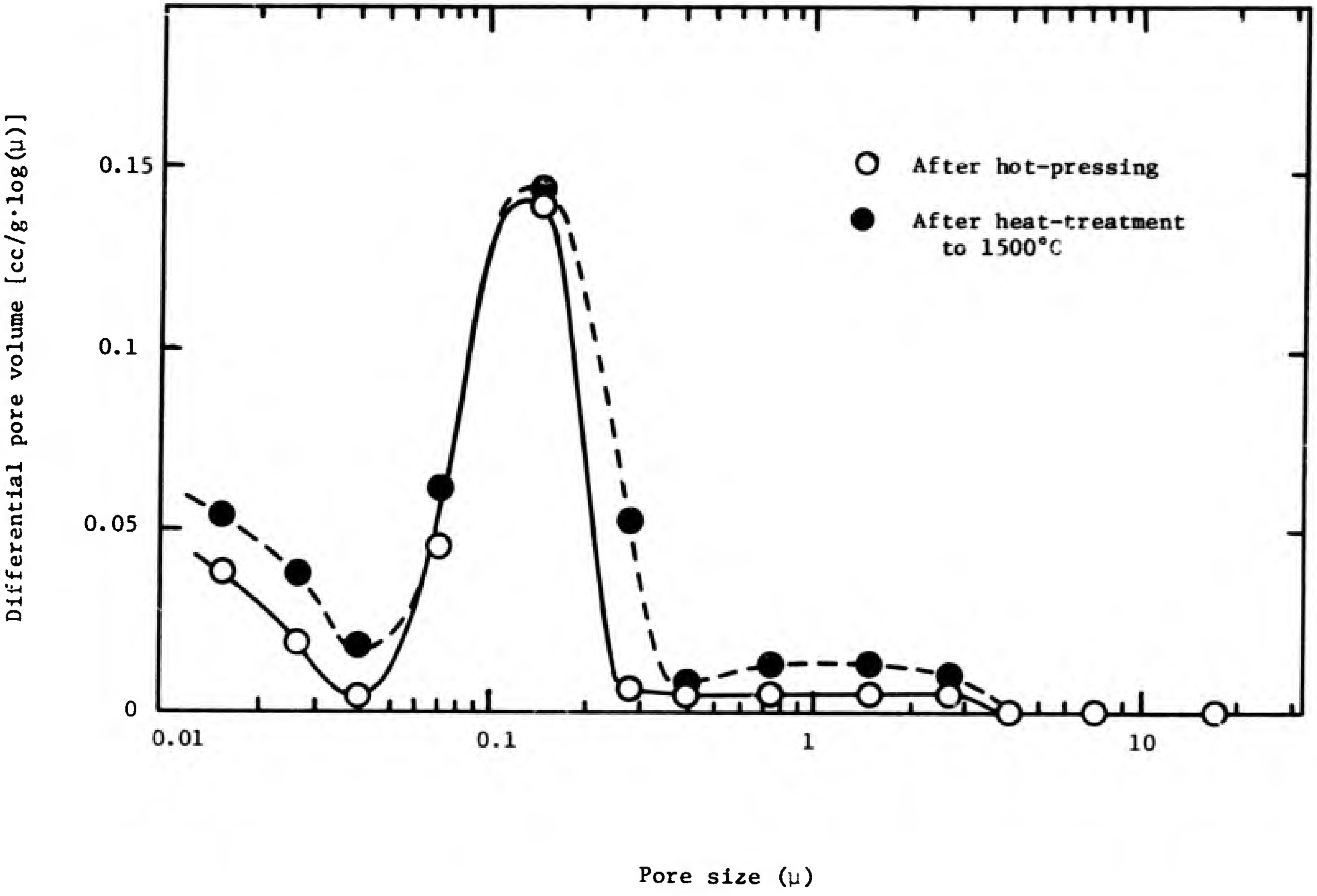

Fig. 1. Distribution of pore size in a specimen of glassy carbon-boron composite (C-B-27) after hot-pressing and heat-treatment to 1500°C.

presumably by the trapping of air bubbles, and thus point to a route through which porosity can be minimized. Figure 2 shows the effect of binder polymer content on the porosity of the specimens after hot-pressing. The filler was 50:50 mixture of glassy carbon/boron, and the binder truxene was polymerized at 440°C for 1 hour. Binder contents of more than 30 w/o did not result in a decrease in the porosity. The excess binder simply flowed out of the die during hot-pressing. It is concluded that the optimum content of binder polymer is 30 w/o, which corresponds approximately to 40 w/o of the content of monomer truxene on account of the weight loss during the polymerization.

Specimens containing different amounts of boron were prepared by mixing with 40 w/o of monomer truxene and subsequent polymerization at 460°C for 1.5 hours followed by hot-pressing and heat-treatment to 1500°C.

Table 2 shows densities and porosities of these specimens after the final heat-treatment. It was note-worthy that all the boron-containing

TABLE 2

DENSITIES AND POROSITIES OF GLASSY CARBON-BORON CARBIDE COMPOSITES

Specimen Number	Initial Composition G.C. (w/o)	B (w/o)	Estimated final composition[a]	Density (g/cc)	Porosity (%)
C-21	60	0	100 w/o G.C.	1.51	4.0
C-B-32	45	15	G.C. - 28 w/o B_4C	1.48	9.5
C-B-29	30	30	G.C. - 50 w/o B_4C	1.60	8.8
C-B-33	15	45	G.C. - 76 w/o B_4C	1.67	18.8
C-B-31	0	60	B_4C - 17 w/o B[b]	1.70	31.4

a) Estimated according to X-ray study and also on the assumption that the weight losses of the specimens are solely attributed to the process of formation of glassy carbon from binder.

b) The amount of excess B present in the form of solid solution is not certain

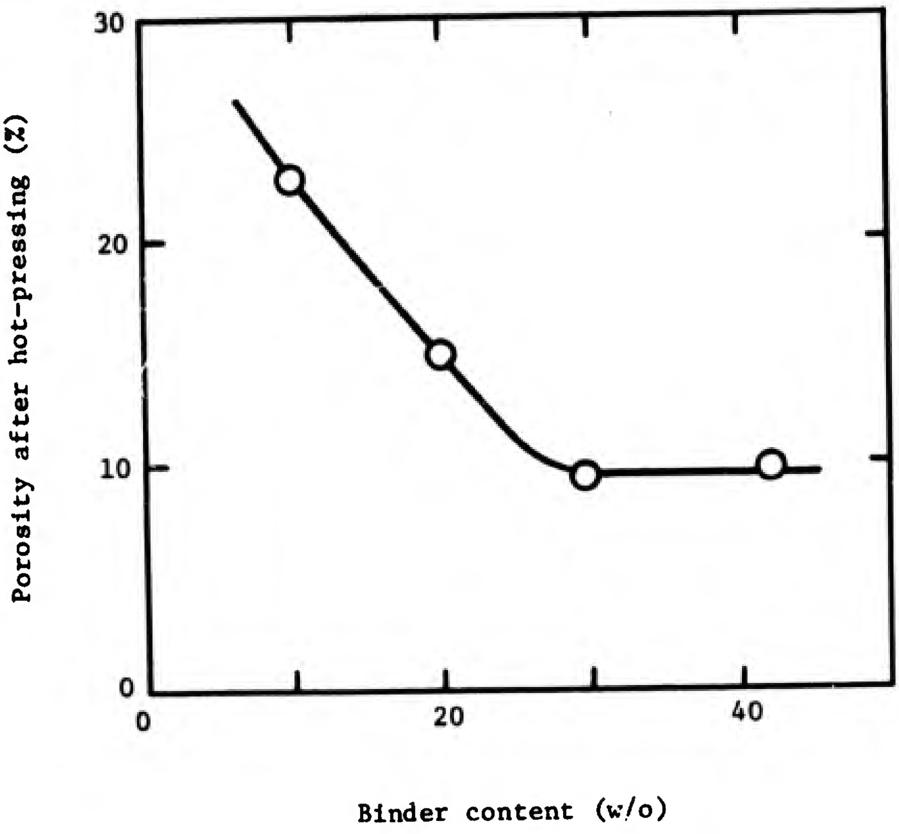

Fig. 2. Effect of binder content on the porosity of the specimens after hot-pressing.

specimens showed sharp pore distributions around 0.1μ similar to Figure 1, while the pores found in C-21 were mostly macroscopic pores larger than 5μ with negligible amount of those around 0.1μ. The porosity is observed to increase with boron content. It is reasonably attributed to the volume change of the carbon-boron system by the formation of boron carbide.

1.3.2 Abrasive wear resistance and hardness

The diamond indentations produced on C-21 and Tokai's glassy carbon showed elastic or anelastic recoveries as reported previously by other workers (22-24). Not only did the indentations lack a regular rhombic shape but also their length decreased in time. The measurements were therefore carried out immediately after the removal of the indentor. The microhardnesses of the present composite specimens showed distributions to certain degrees, although the indentations produced on the surfaces sufficiently covered the inhomogeneous grains of the specimens.

Table 3 shows the abrasive wear resistances and Knoop microhardnesses of the samples. It is found that the present composite materials have higher abrasive wear resistances and higher hardnesses than the steels and the carbon-aluminum alloy composite. Sample C-21 has approximately the same hardness as commercial glassy carbon, though the abrasive wear resistance is somewhat lower. The wear resistance and hardness are found to increase with boron content probably due to the high modulus of boron carbide in spite of the increase of porosity shown in Table 2.

1.3.3 Microstructures investigated by scanning electron microscope

Figures 3a and 3b show the scanning electron micrographs of the polished surface of specimen C-21 at magnifications of X500 and X2,000. The surface is quite smoothly polished and no grain boundaries are observable except macroscopic closed pores. The original filler carbon particles are bonded completely with the matrices of the binder glassy carbon to form a single continuous phase.

TABLE 3

ABRASIVE WEAR RESISTANCE AND KNOOP MICROHARDNESS

Specimen	Abrasive wear resistance (min/10μ abrasion)	Knoop hardness (kg/mm^2)
Stainless steel	1.38 ± 0.02	190 ± 4
Tool steel	1.93 ± 0.11	251 ± 10
C-Al composite	2.65 ± 0.07	249 ± 14
Tokai's glassy carbon	5.83 ± 0.22	316 ± 11
C-21	4.52 ± 0.42	308 ± 17
C-B-32	4.84 ± 0.60	353 ± 46
C-B-29	6.19 ± 0.33	435 ± 73
C-B-33	7.27 ± 0.53	446 ± 65
C-B-31	10.19 ± 0.50	586 ± 49
Corundum	71.0 ± 2.7	1857 ± 44

Figure 4a shows the polished surface of specimen C-B-31 containing hardness indentations at a magnification of X500. A single continuous phase is found again. Figure 4b shows the micrograph of the same specimen at X10,000. It is observed at this magnification that the surface is quite rough and contains a number of small dark spots. It is reasonably speculated that these dark spots correspond to the porous structures which were detected earlier by porosimetry. The conclusion can be drawn that the specimen C-B-31 is composed of B_4C containing homogeneously dispersed fine pores. This conclusion reasonably explains the fact that the hardness of the specimen shown in Table 3 is much lower than the literature value of B_4C (25), 2, 100 kg/mm^2.

Figures 5a and 5c show the micrographs of the polished surfaces of specimens C-B-32, 29, and 33 at a magnification of X500. It is found

(a) X500, 70°.

(b) X2,000, 70°.

Fig. 3. Scanning electron micrographs of the polished surface of specimen C-21 (100 w/o G.C.).

(a) X500, 70°.

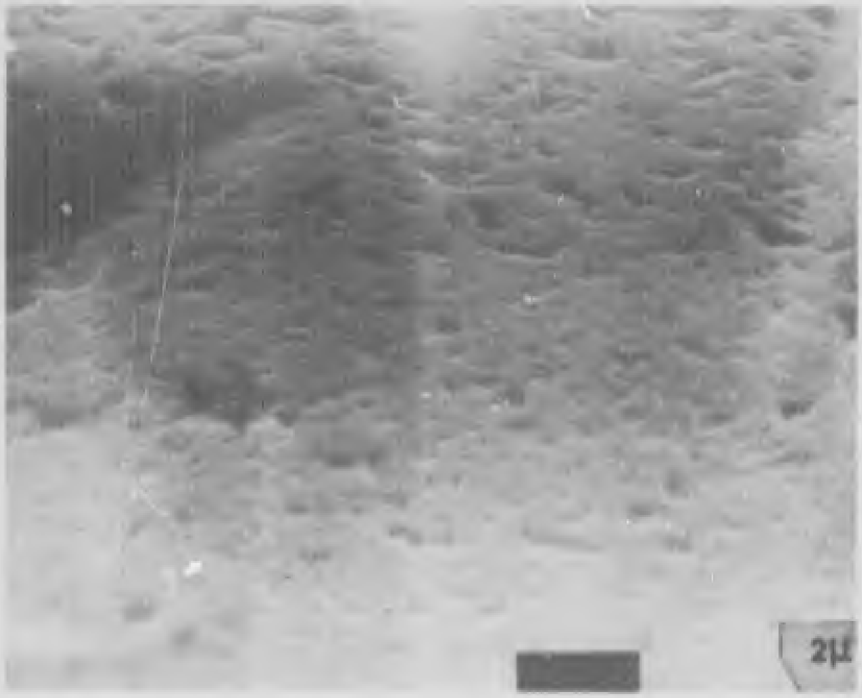

(b) X10,000, 70°.

Fig. 4. Scanning electron micrographs of the polished surface of specimen C-B-31 (B_4C - 17 w/o B).

(a) C-B-32 (G.C. - 28 w/o B_4C), X500, 5°.

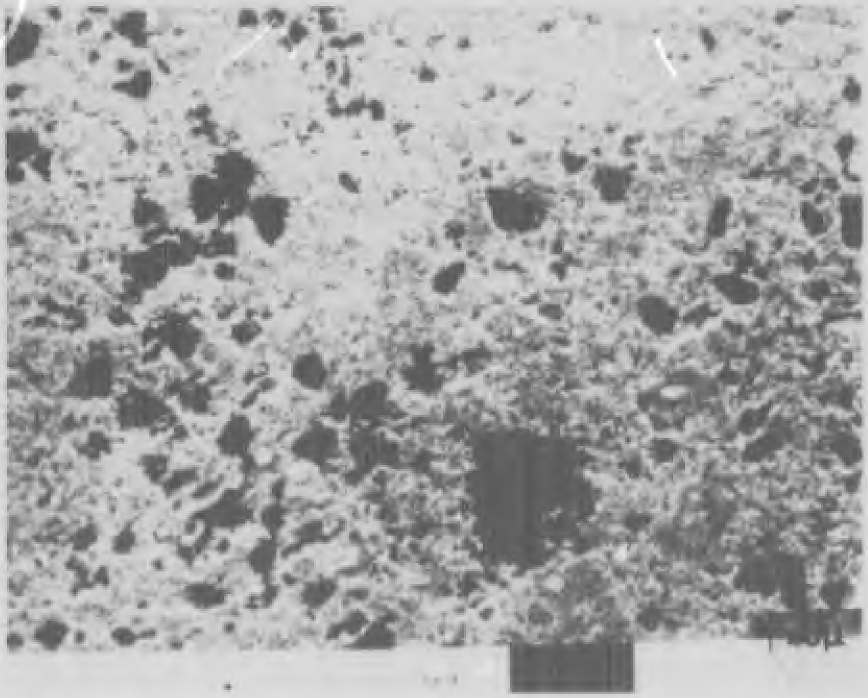

(b) C-B-29 (G.C. - 50 w/o B_4C), X500, 5°.

Fig. 5. Scanning electron micrographs of glassy carbon-boron carbide composites.

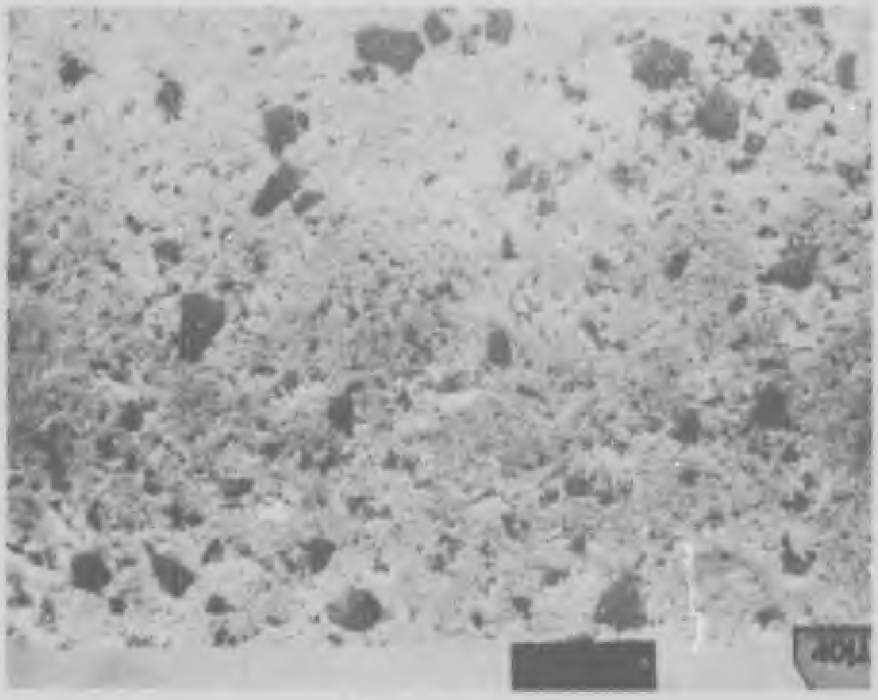

(c) C-B-33 (G.C. - 76 w/o B_4C), X500, 5°.

Fig. 5. Scanning electron micrographs of glassy carbon-boron carbide composites.

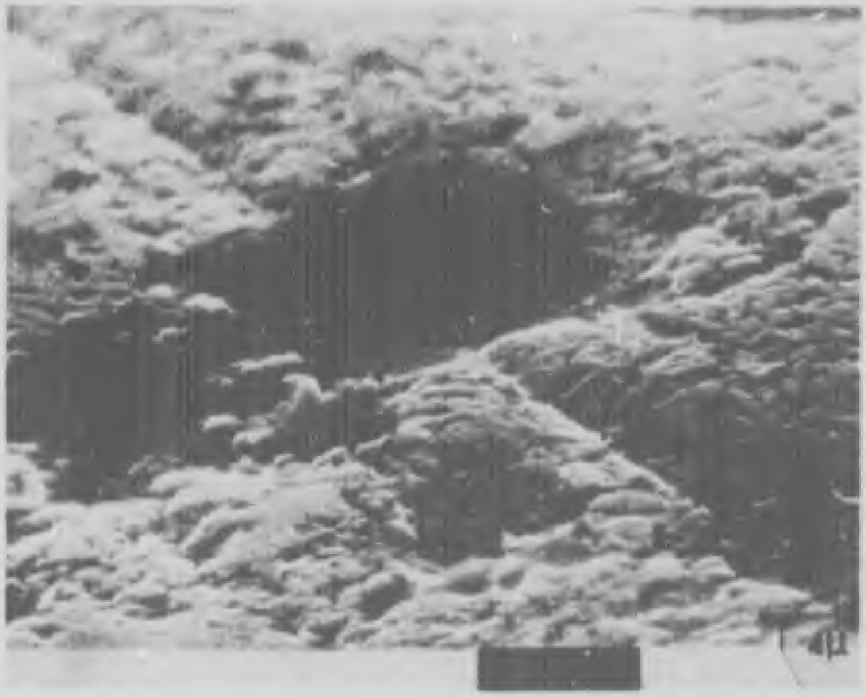

Fig. 6. Scanning electron micrograph of specimen C-B-29. X5,000, 70°.

that these specimens are composed of two phases, and that the fraction of the darker phase decreases with the increase in boron content. The dark particles are considered to correspond to glassy carbon and the bright matrices to boron carbide. The most important factor which affects the contrast between phases of different chemical compositions in the scanning electron micrograph is the secondary electron emission yield. Although such data for glassy carbon and B_4C are not available, it might be reasonably assumed that the latter has higher yield than the former because many electrical insulators are known to have higher secondary electron emission yields than conductors (26).

It is note-worthy that the boron carbide phase forms continuous networks as matrices even at low boron content (C-B-32), while the glassy carbon is found as discontinuous particles dispersed in the former. Some of the glassy carbon particles in the specimens, particularly in C-B-32, are much larger than the original filler particles, and are therefore assumed to be formed by bonding of the filler with binder. It is considered that the binder phases bonded with the filler carbon particles deformed and rearranged their structure in the process of the formation of glassy carbon, forming discontinuous closed phases as a result of surface tensions, and that on the contrary, the phases containing boron continued to retain their rigid network structures. The fractions of glassy carbon particles observed on the surfaces are apparently lower than those estimated from the bulk compositions, and also their surfaces are much rougher than C-21 and C-B-31. The polishing of the composites containing boron carbide against alumina, is considered to have resulted in the scraping off of a large fraction of the relatively soft glassy carbon particles.

Figure 6 shows the micrograph of the surface of C-B-29 at a higher magnification. It is found that there is excellent bonding between particles and the matrix. The glassy carbon particles appear to have lower abrasion resistance than the matrices. The material composing the network of matrices is considered to be porous B_4C similar to C-B-31. This observation coincides with the result that both the abrasive wear resistance and the porosity of the specimens increase with boron content. The Knoop hardness indentation produced across a glassy carbon particle apparently showed the anelastic recovery on it.

1.4 References

1. Harada, Y., NASA-CR-507 (1966).
2. Davidson, K. V., Riley, R. E. and Taub, J. M., LA-3569 (1966), LA-3652 (1967); Riley, R. E., Richerson, N. K. and Schell, D. H., LA-4077 (1968); Riley, R. E., LA-5147 (1973).
3. White, J. L. and Price, R. J., Carbon, 2, 327 (1965); White, J. L. and Pontelandolfo, J. M., Carbon, 4, 305 (1966); ibid. 6, 1 (1968); White, J. L. and Koyama, K., J. Amer. Ceram. Soc. 51, 394 (1968).
4. Matthews, R. B., Fischbach, D. B. and Jenkins, G. M., 3rd Conf. Ind. Carbons Graphite, 515 (1970).
5. Morgan Crucible Co., Ltd., Ger. Patent 1,077,132 (1960).
6. Steinberg, M. A., U. S. Patent 2,979,813 (1961); ibid. 2,979,814 (1961).
7. Micaud, G. and Galy, A., U. S. Patent 3,362,817 (1968).
8. Moore, A. W. and Volk, H. F., U. S. Patent 3,584,370 (1971).
9. Sandstrom, D. J., 9th Conf. Carbon, 19 (1969).
10. Imprescia, R. J., Wewerka, E. M., Reiswig, R. D. and Levinson, L. S., LA-DC-72-1404 (1972).
11. Ford Motor Co., Ltd., Brit. Patent 958,376 (1964).
12. Bonne, R., Jacquot, M. and Fourre, J., Fr. Patent 1,526,317 (1968).
13. Lanza, F., Burg, H., Giuliani, S., Hoepper, M. and Marengo, G., 3rd Conf. Ind. Carbons Graphite, 405 (1970).

14. Couach, M., Ger. Offen. 2,058,239 (1971)

15. Miyata, J., Morimoto, T. and Yamazoe, H., Ger. Offen. 2,034,896 (1971).

16. Katz, R. N. and Gazzara, C. P., J. Mat. Sci. 3, 61 (1968).

17. Yajima, S. and Hirai, T., J. Mat. Sci. 4, 416 (1969); ibid. 4, 424 (1969); ibid. 4, 685 (1969); ibid. 4, 692 (1969).

18. Tukovic, A. and Marinkovic, S., J. Mat. Sci. 5, 541 (1970).

19. Kawamura, K., Ryan, T. and Jenkins, G. M., 9th Conf. Carbon, 14 (1969).

20. Kammereck, R., Nakamizo, M. and Walker, P. L. Jr., Carbon, 12, 281 (1974).

21. Yajima, S. and Omori, M., Chem. Letters, 1, 843 (1972).

22. Cowland, F. C. and Lewis, J. C., J. Mat. Sci. 2, 507 (1967).

23. Jenkins, G. M., Kawamura, K. and Ban, L. L., Proc. Roy. Soc. London, Ser. A 327, 501 (1972).

24. Dobbs, H. S., J. Phys. D. 7, 24 (1974).

25. Tarosov, L. P. and Thibault, N. W., Trans. Am. Soc. Metals, 38, 331 (1947).

26. Oatley, C. W., "The Scanning Electron Microscope" (1972), Cambridge University Press, Cambridge, England.

2. CELLULOSE CARBON-CVD COMPOSITES

(S. Marinkovic, P. W. Whang, A. Navarette, and P. L. Walker, Jr.)

2.1 Introduction

Carbon-carbon composites are of increasing interest particularly for aerospace applications. The most common approach at producing these materials is to infiltrate woven carbon fiber structures by the chemical vapor deposition (CVD) of carbon from a hydrocarbon gas. Such an approach has been reviewed in detail by Kotlensky (1). Alternatively, compacted carbon particles which are more or less weakly bonded together can serve as a substrate for the addition of carbon by chemical vapor deposition. In this study porous cellulose carbon artifacts fabricated from micron-sized cellulose powder served as the substrate for the production of carbon-carbon composites. Cellulose has the virtue for this application of having a low carbon yield upon carbonization (about 18% by weight). Hence, an artifact of high open porosity can be produced which lends itself to large additions of a second phase -- like CVD carbon.

2.2 Experimental

2.2.1 Preparation of Uninfiltrated Artifacts

Cellulose powder obtained from Applied Science Laboratory, Inc. has been used as a starting material. The powder had a particle size range from 2 to 27μ with a maximum in the distribution at 12μ. From water adsorption measurements, it is estimated to have a crystallinity content of 74% by weight (2).

In order to establish optimum conditions for the fabrication of cellulose carbon artifacts to be used as substrates for CVD infiltration, an extensive study of the influence of molding pressure and heating cycle on properties of artifacts was made. Bars 5 cm long by 0.50 cm wide by 0.45 cm thick were prepared using molding pressures ranging from 2500 to 50,000 psi. These bars were initially cured and carbonized under conditions previously reported (3). These experiments have shown that closed porosity is increased and open porosity is reduced with increasing molding pressure. That is, with an increase in molding pressure from 2500 to 50,000 psi open porosity decreased from 57.1% to 6.7% while closed porosity increased from 12.0% to 30.1%. Apparent density of the artifacts increased from 0.68 g/cc to 1.39 g/cc. The theoretical infiltration density (TID) calculated according to Kotlensky, assuming a density of 2.1 g/cc for the CVD carbon, would increase from 1.47 g/cc for artifacts prepared at 50,000 psi to 1.85 g/cc for artifacts prepared at the lowest molding pressure. A molding pressure of 3000 psi was selected for the preparation of all samples to be reported on.

Experiments were directed to establish effects of curing temperature and heating rate up to the maximum temperature (800°C) on the quality of the artifacts produced. Samples were packed in carbon black and heated under 1 atm of N_2. Upon heating to 800°C, the cellulose powder undergoes a weight loss of about 82%. However, most of this weight loss occurs during the primary degradation process which starts at about 250°C. The most critical part of the thermal cycle involves allowing an extended curing time at about 250°C. If this was not done, substantial bending and cracking of the samples occurred. The cycle standardized upon was: heating to 150°C at a rate of 2°C/min, then at 1.4°C/min to 250°C, curing for 20 hr at 250°C, heating at 1.7°C/min to 300°C, at 2.4°C/min to 500°C, at 4.5°C/min to 800°C, and finally soaking at 800°C for 1 hr. The total elapsed time for the curing and heating cycle was 30 hr.

2.2.2 Infiltration Conditions

A 50% propylene-50% helium mixture was used at atmospheric pressure for infiltration. On the basis of a number of experiments, 700°C was chosen as a desirable infiltration temperature. At this temperature samples can be infiltrated for 72 hr without any noticeable external surface deposition. Higher temperatures lead to an increased surface deposition and formation of an impervious coating before the porous body is filled with carbon to the desired density.

The gas mixture passed in laminar flow through the reactor, it having a residence time of 4 min in the hot zone. Prior to its introduction, it was dried by passage over P_2O_5 and $CaCl_2$. In order to rapidly establish the desired gas composition in the unit when commencing a deposition run, the entire system was evacuated of helium (used during heat up) prior to introduction of the propylene-helium mixture. A three zone furnace was employed to obtain a hot zone 18 in long and 7.5 cm in diameter in which the temperature could be maintained within ± 2°C. Up to twenty samples could be infiltrated at one time.

2.2.3 Heat Treatment Procedure

Some samples infiltrated at 700°C were further heat treated to higher temperatures under 1 atm of helium using a graphite resistance furnace. Samples were heated to the desired temperature at a rate of 10°C/min and held at final temperature for 1 hr.

2.2.4 Measurement of Sample Properties

Densities were determined by several methods. Apparent densities were determined from the weight and dimensions of the samples. Mercury densities were determined by mercury displacement at a pressure of 1 atm. In selected cases, density was also determined by methanol displacement at 25°C using a pycnometer.

Pore size distributions were measured using a mercury porosimeter up to a pressure of 1000 atm, which is equivalent to a pore diameter of 140A.

Flexural strengths were measured by a three-point bending test using the Instron universal testing machine.

Young's modulus was determined from the resonant frequency of flexural vibration, using a Namettre Company acoustic spectrometer.

Knoop microhardness was determined using a Leitz miniload hardness tester. In order to make indentations more visible, the polished cross-sectional surface of the sample was coated prior to testing with a thin aluminum film (200A).

Wear resistance was determined using a standard polishing machine. Samples with approximate planar dimensions of 9x3 mm were pressed by a 740 g load onto silicon carbide abrasive paper No. 320 located at a distance 2.5 cm from the center of the polishing disc. They were abraded using a fixed number of revolutions of the abrasive paper at a speed of 180 turns/min in flowing water. Weight loss per 500 revolutions was taken as a measure of wear resistance. For comparison, wear resistance of stainless steel (Fe-18 Ni-13 Cr-2 Mo), sintered alumina (density 3.84 g/cc), and Tokai glassy carbons were also measured.

Oxidation resistance was measured using a Fisher TGA apparatus. Samples were heated in a stream of N_2 up to a desired temperature (500°C for most samples and 600°C for the more oxidation resistant). After 15 min, during which the temperature stabilized, air was admitted at a rate of 200 cc/min. The weight of the sample was continuously recorded as a function of time until 70-80% of the initial weight was consumed. Curves of burn-off versus time were used to determine the maximum rate of oxidation, $R_T = dw/w_o dt$ where w_o is the initial sample weight.

Interlayer spacing, C/2, and crystallite height, L_c, were determined using an x-ray unit consisting of a Picker generator and Siemens goniometer. The C/2 was determined from the peak position and L_c from the width at half maximum of the (002) reflection recorded at a goniometer speed of 0.5° (2θ)/min using nickel-filtered copper radiation.

The coefficient of thermal expansion (CTE) in the 100-400°C temperature range was determined using a DuPont 942 Thermomechanical Analyzer.

Electrical resistance was measured employing a potential probe method which utilized two extra electrodes to eliminate errors due to contact resistance.

Surface areas were determined from N_2 (77°K) and CO_2 (298°K) adsorption measurements using a volumetric-type apparatus. An equilibration time of 30 min was allowed for each adsorption point. Surface areas were calculated using the BET equation for N_2 and the Dubinin equation (4) for CO_2. Molecular areas of $16.2A^2$ and $25.3A^2$ were taken for N_2 and CO_2, respectively.

2.3 Results and Discussion

2.3.1 Properties of Samples Infiltrated for Various Times

Following curing and carbonization of the uninfiltrated samples, their dimensions decreased to 3.5 cm long, 0.37 cm wide, and 0.30 cm thick This represents a volume shrinkage over the original compacted cellulose powder of 65%.

With increasing infiltration time, apparent density of the samples increased as their porosity decreased. It may be expected that for a given set of conditions the rate of infiltration at time t should be proportional to the open porosity (θ) present in the sample at that time. Hence

$$-\frac{d\theta}{dt} = k\theta \tag{1}$$

where the rate of infiltration is expressed as the rate of decrease of open porosity. From equation (1) it follows that

$$\log \frac{\theta_t}{\theta_o} = -\, k't \tag{2}$$

or if the remaining open porosity at time t, θ_t, is expressed as a percentage of the initial porosity θ_o

$$\log\,(100\ \theta_t/\theta_o) = 2 - k't \tag{3}$$

A plot of log (100 θ_t/θ_o) vs time, shown in Figure 1, confirms the assumed linear relationship between log θ_t and t (although the extrapolated straight line intersects the porosity axis at 1.95 instead of 2.0). The infiltration rate constant obtained from the slope equals $-\ 0.00877\ \text{hr}^{-1}$. For example, to reduce the open porosity by a factor of two, infiltration need last about 34 hr. It should be emphasized that open porosity was taken as that in voids down to 140A, that is the size filled by mercury at 1000 atm pressure. Close agreement between mercury and methanol densities indicated that the amount of open porosity present in voids less than 140A in diameter in the artifact was small.

Figure 2 shows that the open porosity decreases linearly with increasing apparent density of the infiltrated samples, following an initial sharp decrease in porosity at low infiltration levels. From the slope of the straight line and from the fact that there is a negligible change in volume of the artifacts, the CVD carbon is estimated to have an apparent density of 1.64 g/cc.

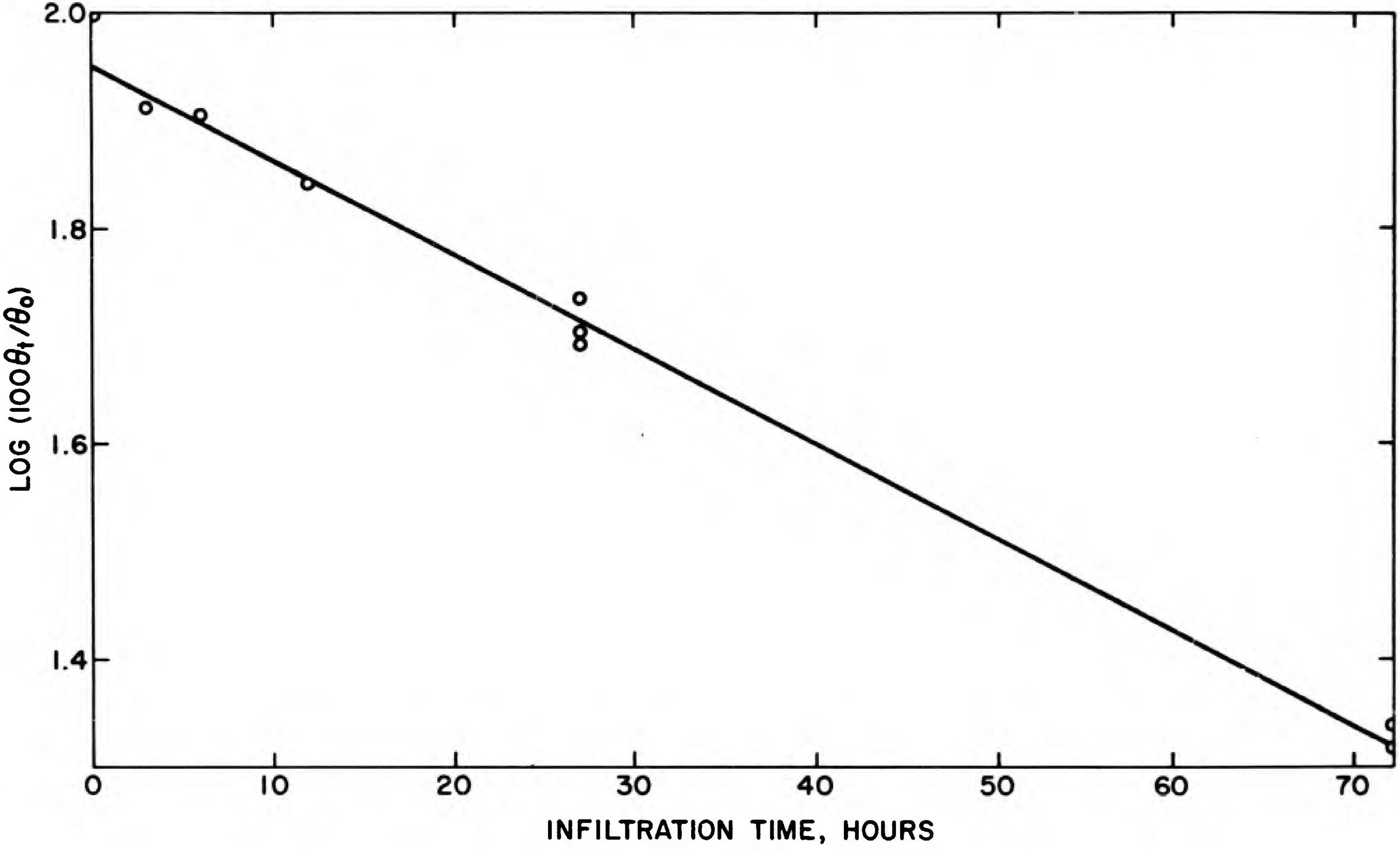

Fig. 1. Change of open porosity expressed as percent of initial open porosity with time of infiltration of cellulose carbon artifacts.

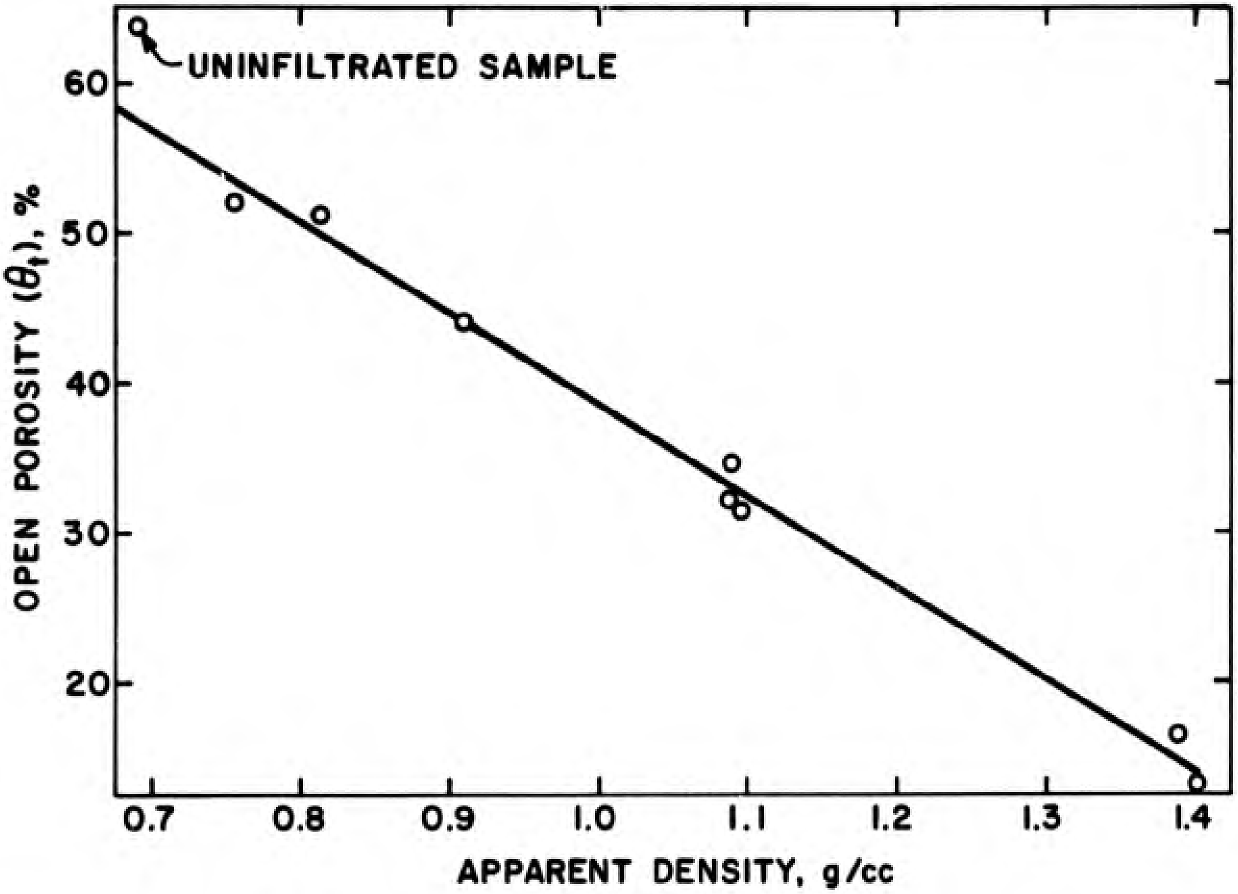

Fig. 2. Change of open porosity with change in apparent density of cellulose carbon artifacts as a result of carbon infiltration.

Changes in flexural strength (σ), Young's modulus (E), Knoop hardness (H), and electrical resistivity (ρ) with changes in apparent density of the artifacts upon infiltration can be expressed by log-log plots, as seen in Figure 3. In all cases experimental points fit linear plots reasonably well, except for the uninfiltrated sample. The deviation is particularly high in the case of microhardness, which sharply decreases after the initial infiltration and then increases linearly. In going from the uninfiltrated samples to the samples infiltrated for the longest time (72 hr), properties change as follows: flexural strength increases from 100 to 800 kg/cm^2, Young's modulus increases from 1.7×10^4 to 2.0×10^5 kg/cm^2, Knoop hardness increases from 86 to 182 kg/mm^2, and electrical resistivity decreases from 200 to 29 mohm·cm.

In preliminary experiments directed at arriving at a suitable infiltration temperature, some infiltration runs were made at 810°C. It was clear that this temperature produced too rapid a rate of carbon deposition, resulting in blocking of the pores at the exterior surface of the bars and in an extensive increase in dimensions of the artifact as carbon built up on the surface. On selected samples which were infiltrated for 24 hr at 810°C, flexural strength and Young's modulus were measured. Despite the fact that infiltration had increased the apparent density of the artifact to 1.1 g/cc, the flexural strength was essentially unchanged from the value for the uninfiltrated sample, that is 100 kg/cm^2. This is to be compared with the flexural strength of the artifact infiltrated at 700°C to a density of 1.1 g/cc -- that is 430 kg/cm^2. In contrast, infiltration at 700 or 810°C produced similar values of Young's modulus.

The coefficient of thermal expansion increases with increasing infiltration time (or apparent density) as seen in Table 1. Kotlensky

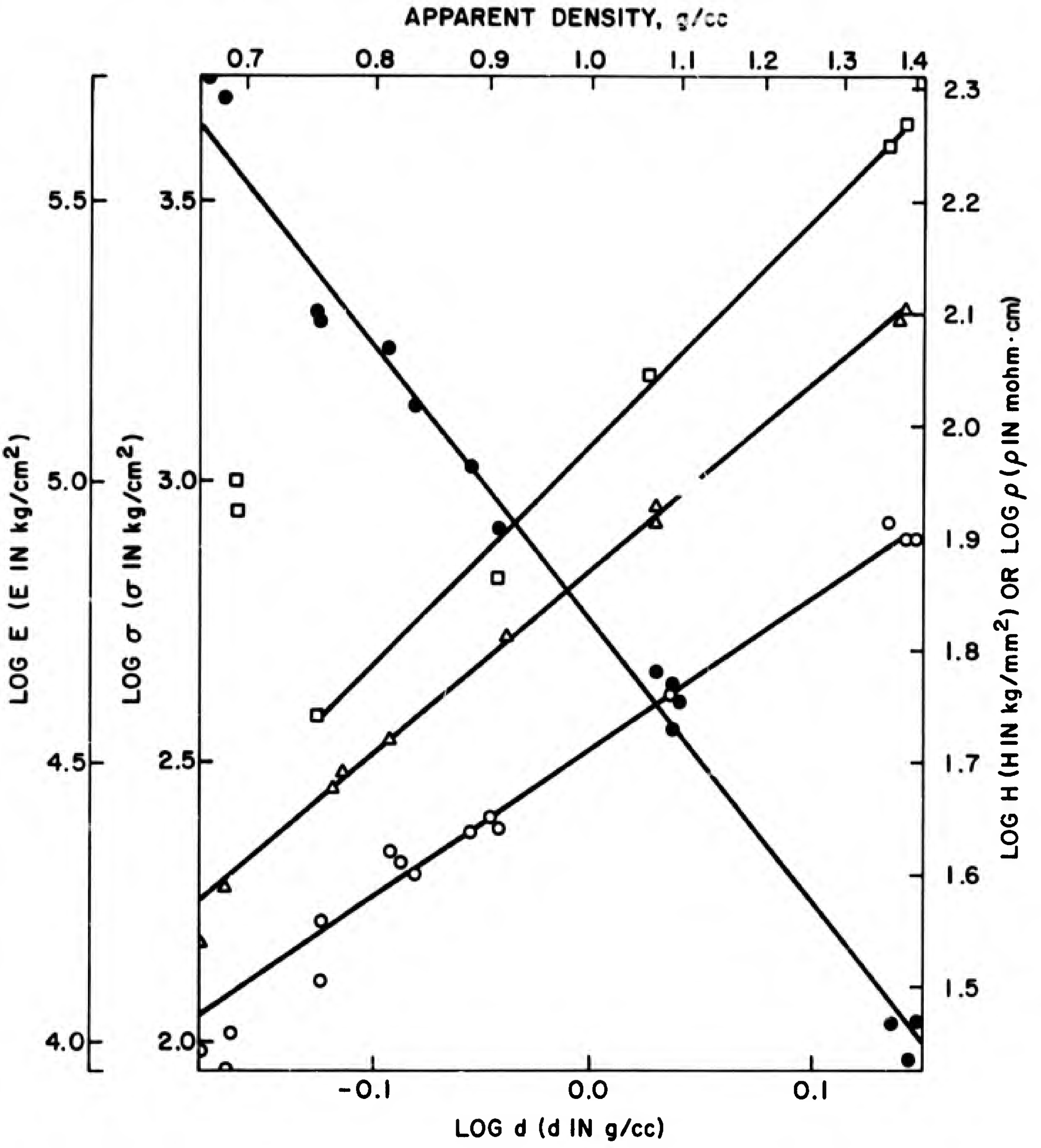

Fig. 3. Dependence of flexural strength (O), Young's modulus (△), Knoop hardness (□), and electrical resistivity (●) upon apparent density of composites.

TABLE 1

WEAR RESISTANCE AND CTE OF INFILTRATED SAMPLES TREATED AT DIFFERENT TEMPERATURES

Infiltration time, hr	HTT °C	Wear mg/500 revol.	CTE X 10^6 $°C^{-1}$
0	No HT	-	1.35
12	No HT	1940	1.52
24	No HT	240	-
72	No HT	3.0	2.53
0	1000	-	0.90
12	1000	804	1.24
24	1000	273	-
72	1000	4.7	2.08
0	1500	-	0.51
12	1500	1012	-
24	1500	400	-
72	1500	8.7	1.39
24	2000	1170	-
72	2000	65	1.39
72	2400	190	1.39

summarizes available CTE data for infiltrated felts and woven samples and shows that there is a wide variation with raw materials and processing conditions (1).

As seen in Table 1, infiltration with CVD carbon markedly improves the wear resistance of the base cellulose carbon. Following infiltration for 72 hr, it wears less rapidly than the stainless steel sample which looses 17.7 mg in 500 revolutions. However, the most fully infiltrated sample still has a wear resistance inferior to alumina (0.60 mg in 500 revolutions).

The x-ray diffraction profile of the cellulose carbon was very diffuse and did not permit an estimate of interlayer spacing or crystallite size. A better defined (002) reflection was observed following infiltration for 72 hr. From this reflection, the CVD carbon is estimated to have an interlayer spacing of 3.54A and an L_c of 15A.

Figure 4 presents reactivity results in air at 500°C. Infiltration of the base cellulose carbon markedly reduces reactivity. In the region of constant (and maximum) oxidation rate, reactivities are 4.1% burn-off/hr for the original artifact, 1.4%/hr following infiltration with CVD carbon for 12 hr, and 0.27%/hr following infiltration for 72 hr. It was possible to follow controlled oxidation out to a burn-off level of 70% on the sample infiltrated 72 hr before spontaneous ignition occurred. On the other two samples, at a burn-off of about 45% spontaneous ignition occurred and the temperature increased in an uncontrolled manner.

The uninfiltrated carbon artifacts have high specific surface areas, that is, areas in CO_2 and N_2 are 1050 and 480 m^2/g. A difference in these areas is indicative of some molecular sieving in pores between 4 and 5A (5). As expected, infiltration for only 3 hr sharply reduces the CO_2 and N_2 areas to 16 and 4 m^2/g. Further infiltration does not have a major effect on specific surface areas.

2.3.2 Effect of Heat Treatment on Properties of Composites

Samples were heat treated at temperatures of 1000, 1500, 2000, and 2400°C. Figure 5 summarizes results on changes in weight, linear dimension and sample density with heat treatment temperature (HTT). It is seen that if the cellulose carbon artifacts are taken to 800°C and if CVD infiltration with propylene is carried out at 700°C, subsequent heat treatment up to 2400°C produces relatively little changes in sample

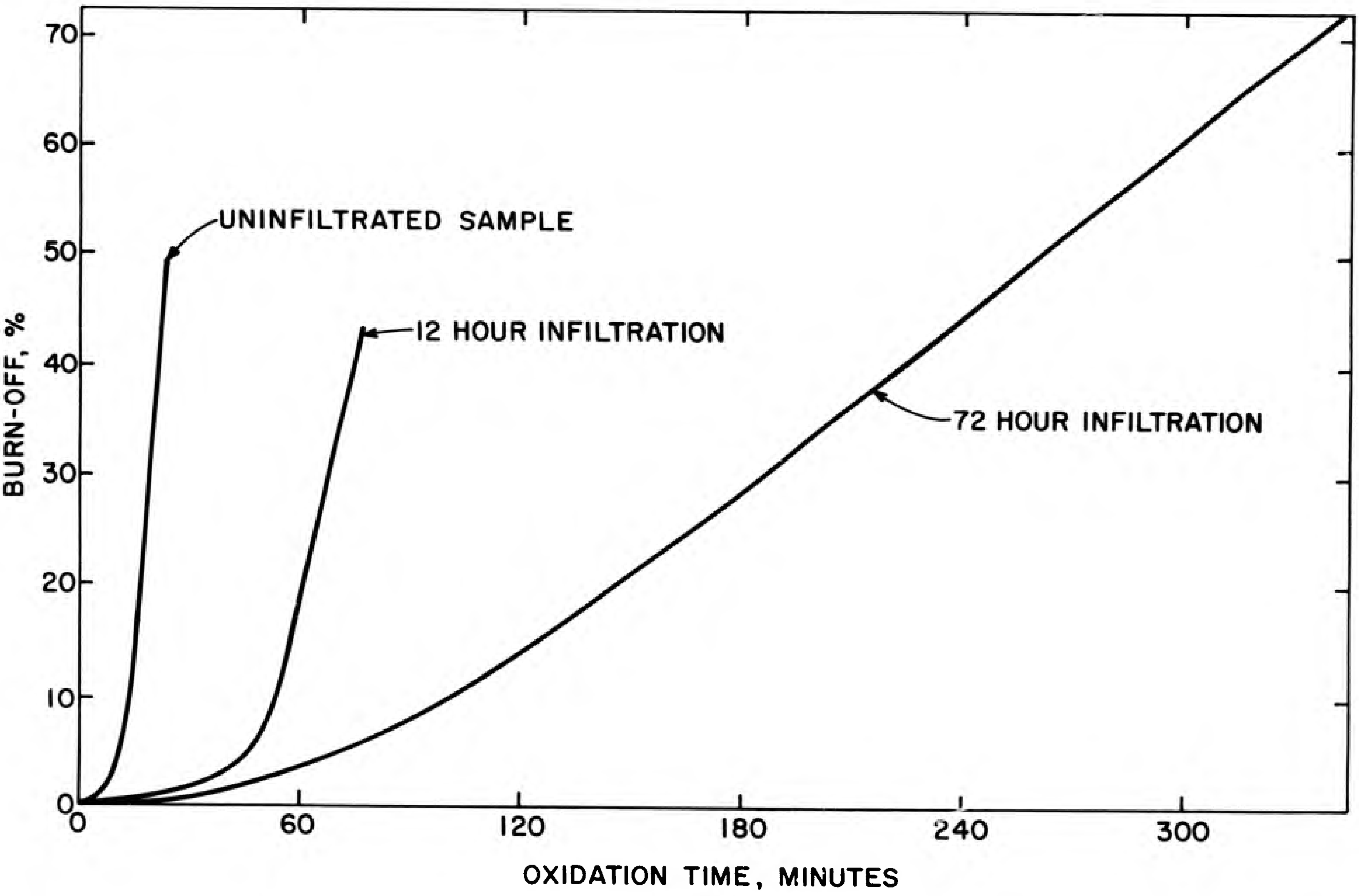

Fig. 4. Reactivity of composites to air at 500°C.

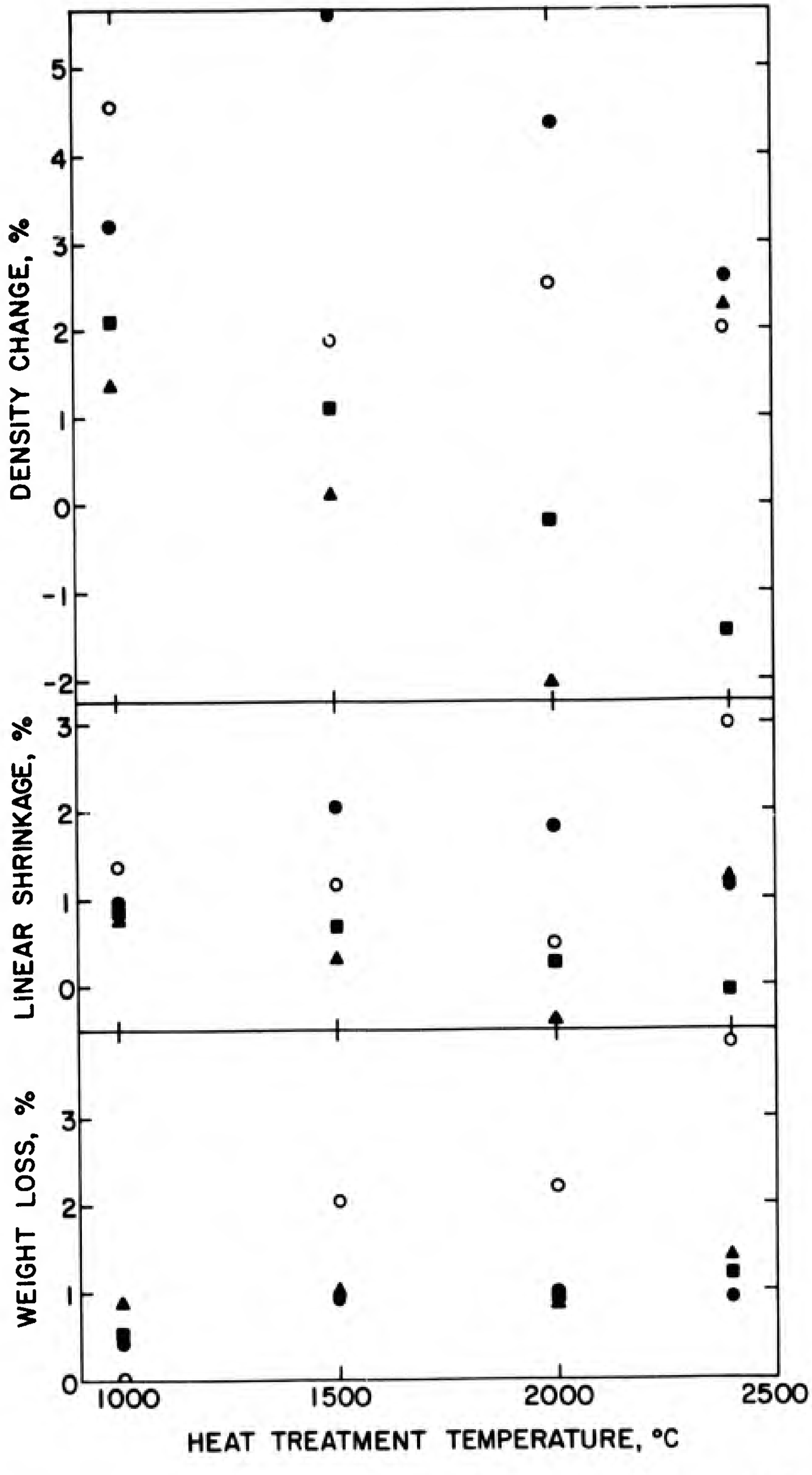

Fig. 5. Weight loss, linear shrinkage, and density change upon heat treatment of composites produced by carbon infiltration for varying times: O, no infiltration; ▲, 3 hr; ■, 12 hr; ●, 72 hr.

weight and dimensions. Changes in dimensions which do occur can be associated primarily with two factors -- shrinkage because of crystallite growth and alignment and expansion because of relaxation of residual stresses and pressure build-up of gases in closed pores.

Table 2 summarizes x-ray diffraction results for both uninfiltrated samples and those infiltrated for 72 hr, followed by heat treatment up to 2400°C. For the uninfiltrated samples, crystallite growth is small, and three dimensional layer plane alignment is negligible for heat treatment up to 2400°C. This is expected for cellulose carbon. For the infiltrated samples, on the other hand, significant crystallite growth of the CVD carbon occurs. Further, interlayer spacing monotonically decreases with increasing HTT such that at 2400°C the spacing indicates significant planar alignment into an ababab registry (6).

TABLE 2

INTERLAYER SPACING AND L_C FOR UNINFILTRATED AND 72 HR INFILTRATED SAMPLES

Sample	HTT, °C	Interlayer Spacing, A	L_c, A
U	None	Too diffuse	
I	None	3.54	15
U	1000	3.79	11
I	1000	3.53	16
U	1500	3.65	13
I	1500	3.50	38
U	2000	3.57	16
I	2000	3.465	94
U	2400	3.435	40
I	2400	3.383	125

Figures 6-9 summarize results for changes in flexural strength, Young's modulus, Knoop hardness and electrical resistivity with increasing HTT for the uninfiltrated samples and those infiltrated at 700°C for

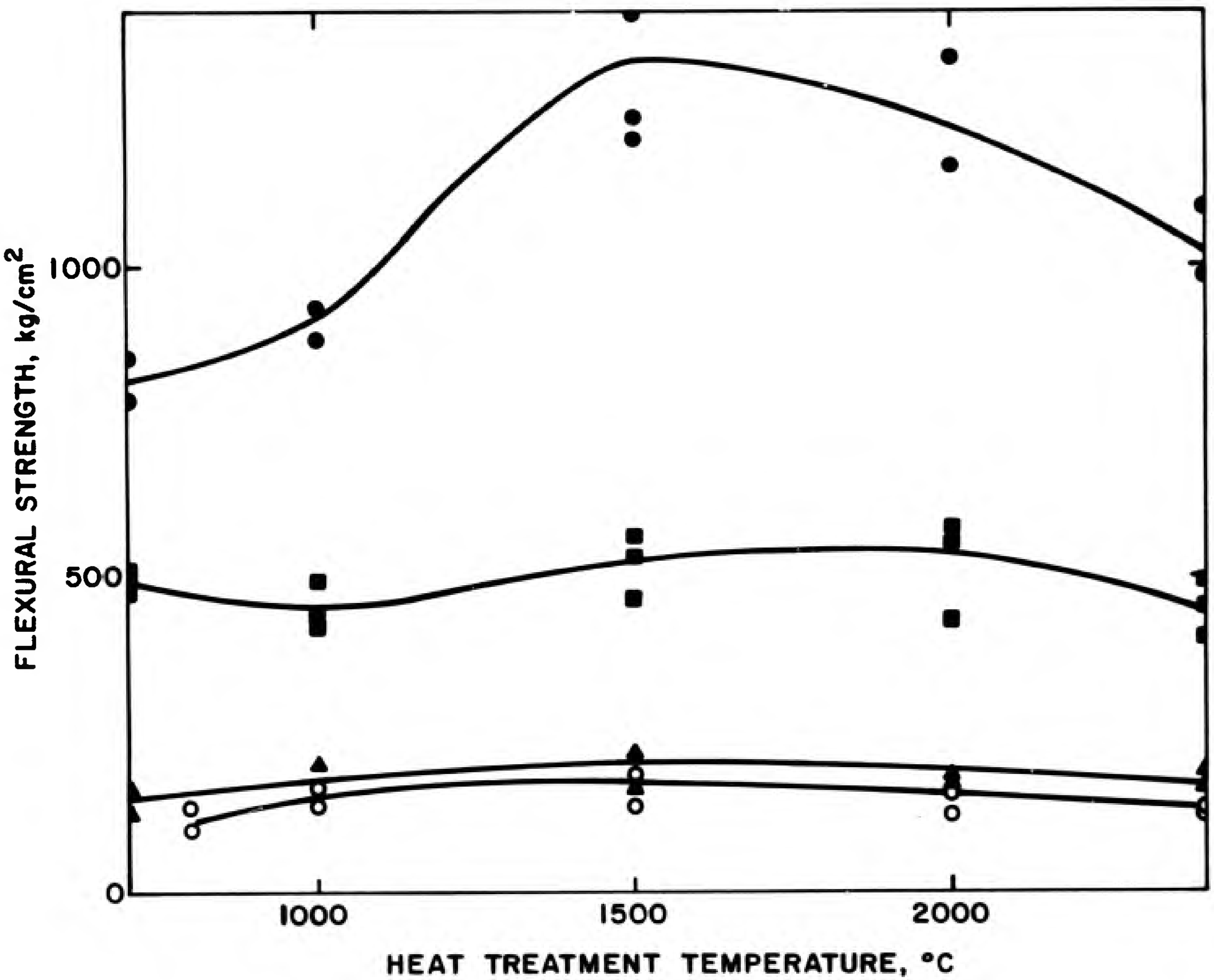

Fig. 6. Change of flexural strength with heat treatment of composites produced by carbon infiltration for varying times: 0, no infiltration; ▲, 3 hr; ■, 12 hr; ● 72 hr.

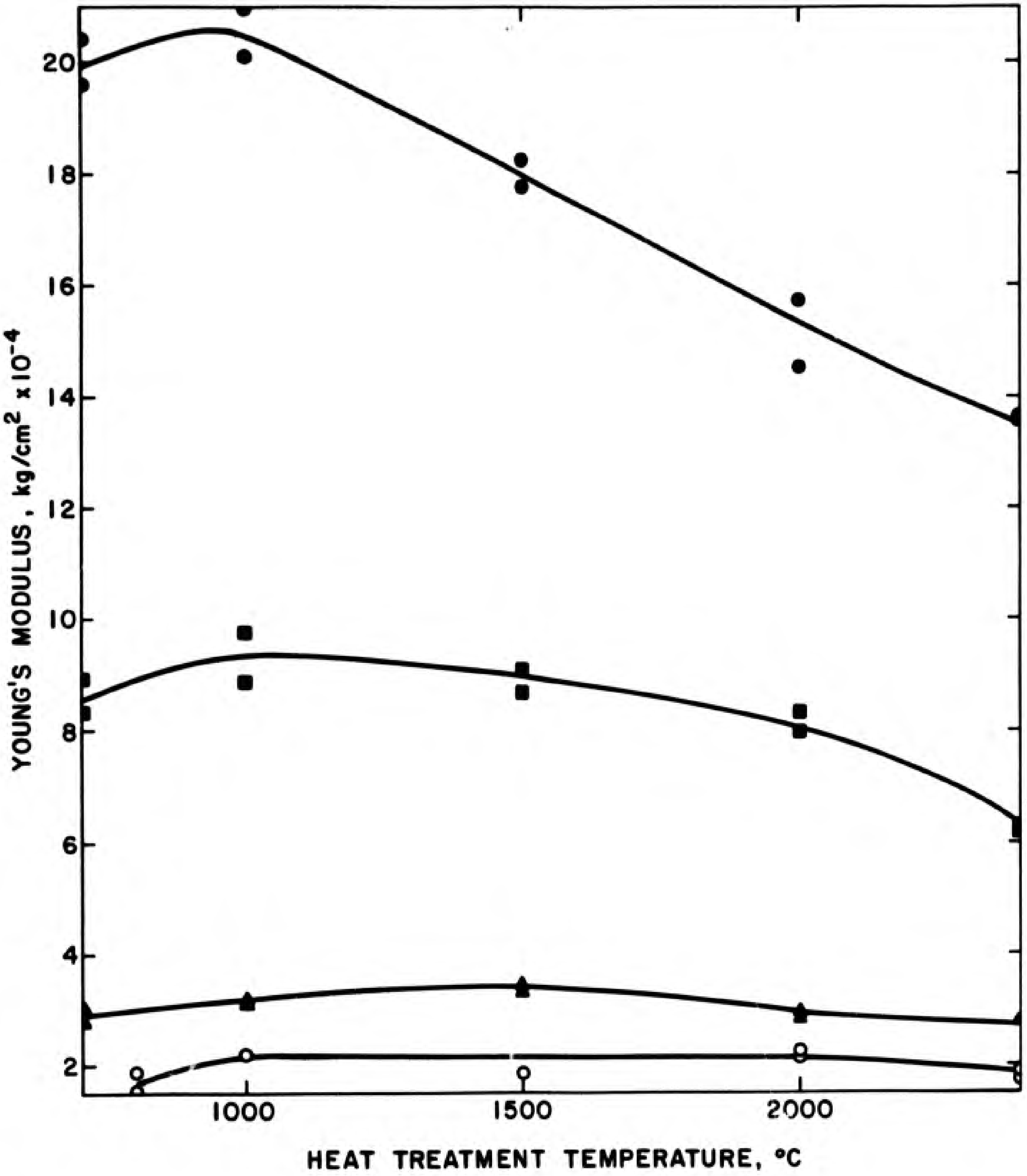

Fig. 7. Change of Young's modulus with heat treatment of composites produced by carbon infiltration for varying times: 0, no infiltration; ▲, 3 hr; ■, 12 hr; ● 72 hr.

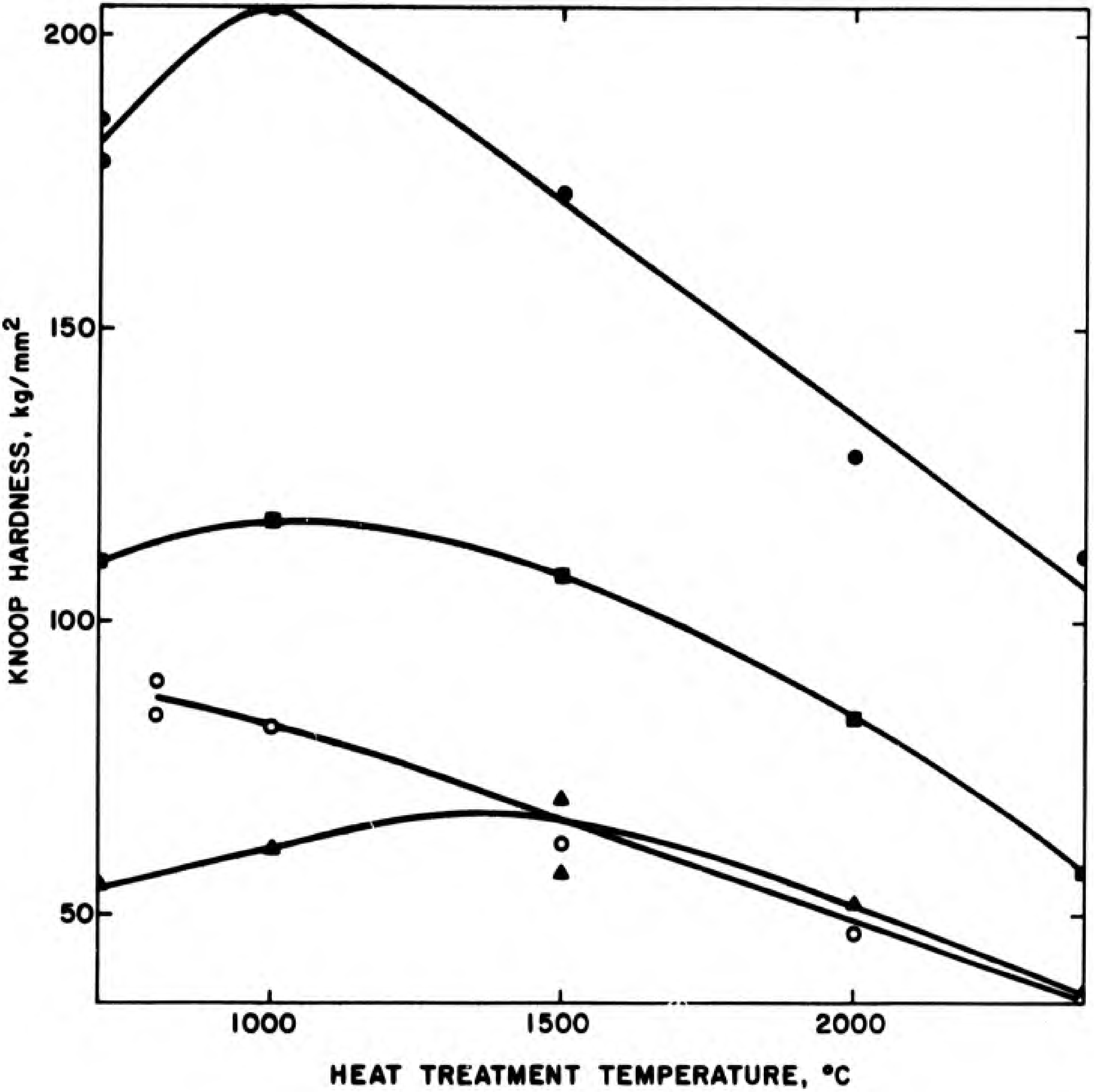

Fig. 8. Change of Knoop hardness with heat treatment of composites produced by carbon infiltration for varying times: 0, no infiltration; ▲, 3 hr; ■, 12 hr; ● 72 hr.

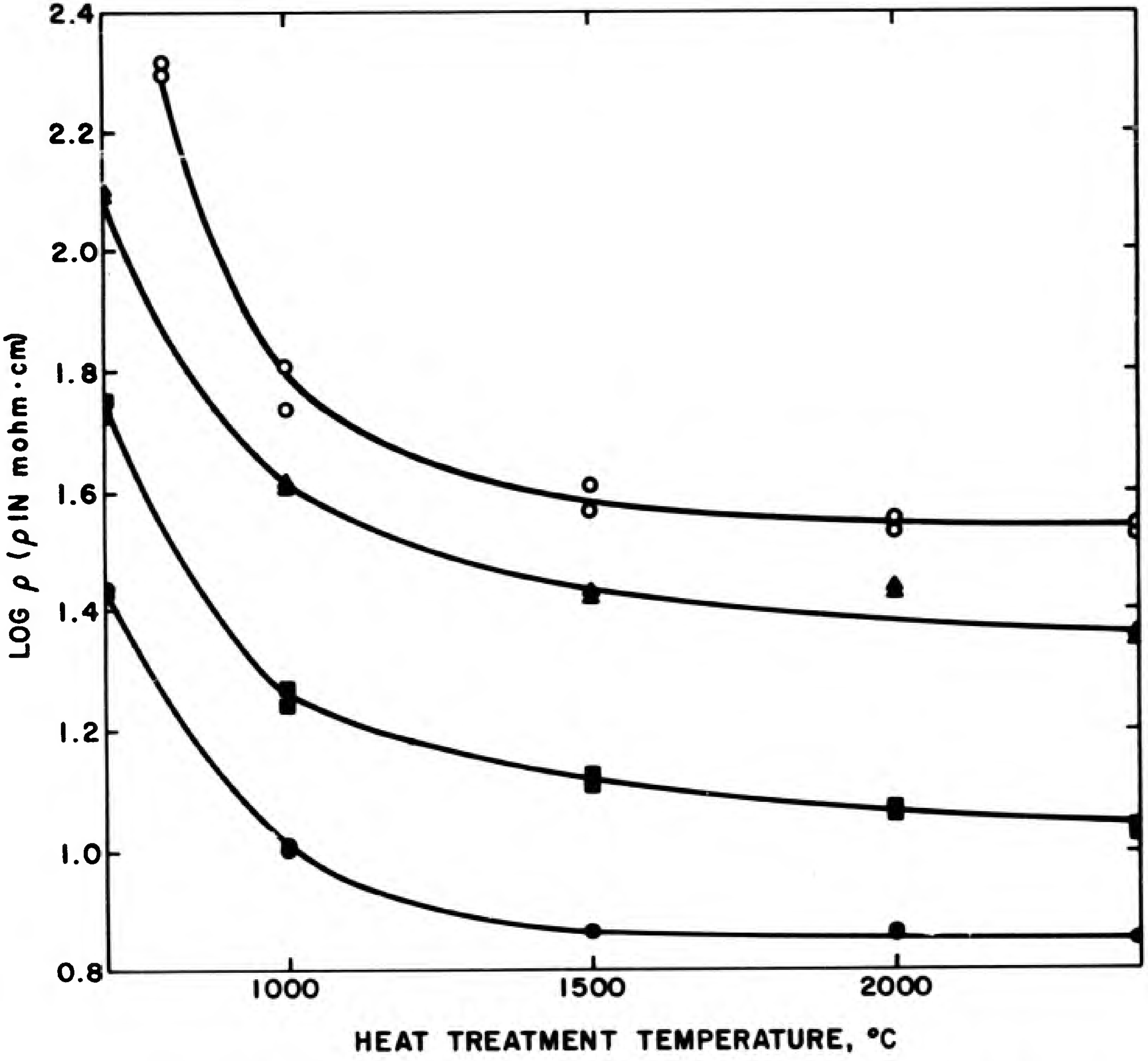

Fig. 9. Change of electrical resistivity with heat treatment of composites produced by carbon infiltration for varying times: 0, no infiltration; ▲, 3 hr; ■, 12 hr; ● 72 hr.

3, 24, and 72 hr. All data points taken are shown on the figures. Heat treatment has relatively little effect on flexural strength or Young's modulus for artifacts infiltrated up to 24 hr. For the 72 hr infiltrated samples, flexural strength goes through a pronounced maximum at about 1500°C HTT and then decreases with further heat treatment. This behavior is analogous to the change of density with HTT. Young's modulus of the 72 hr infiltrated samples goes through a shallow maximum following heat treatment at 1000°C and then decreases continually with further increases in HTT. Knoop hardness of the uninfiltrated samples monotonically decreases with increasing HTT. For the infiltrated samples, hardnesses go through maxima with increasing HTT. In each case, however, the hardness of the composites heated to 2400°C is substantially lower than the hardness of the unheat-treated samples.

As seen from Figure 9, electrical resistivities decrease sharply with increasing HTT. Most of the decrease occurs with heat treatment up to 1500°C and is primarily attributed to removal of hetero-atoms from carbon atoms located at the periphery of small trigionally bonded crystallites (7). The result is the production of positive hole carriers Heat treatment above 1500°C results in little further decrease in resistivity since increase in crystallite size produces two counter-balancing effects -- an increase in carrier mobility but a decrease in number of positive hole carriers.

As is the case for the unheat-treated composites (Figure 3), log-log plots of σ, E, ρ and H versus composite density give straight lines for each HTT. Therefore, log-log plots of E vs σ give straight lines for each HTT, with the slope of the plots decreasing with increasing HTT.

As is seen in Figure 10 heat treatment of the 72 hr infiltrated composite to 1500 or 2000°C markedly reduces reactivity to air over that found for the uninfiltrated sample (Figure 4). Reactivity of the 1500°C heat treated sample was measured at 500°C; whereas because of its very low reactivity, the sample having a HTT of 2000°C was oxidized at 600°C. Decreases in reactivity with increasing HTT generally are attributed to one or more of the following reasons: decrease in active surface area, increase in crystallinity, and decrease in amount of impurities which can act as oxidation catalysts. In this case for the infiltrated samples, CO_2 surface areas, in fact, increased upon heat treatment to 1500°C. However, as discussed previously (8), an increase in total surface area as given by CO_2 adsorption does not necessarily mean that the surface area active to oxidation would also increase. X-ray diffraction studies of some samples following oxidation at 500°C to large burn-offs showed that the carbon remaining had a lower mean interlayer spacing and larger average crystallite height than that contained in the original carbon composites. This is in agreement with previous studies on the gasification of electrode graphite composites (9), that is the less crystalline material is being reacted away preferentially

It is of interest to compare the properties of the carbon-carbon composites prepared in this study with the properties of commercial glassy carbons. In Table 3 properties are compared for the 72 hr infiltrated composites with those of Tokai glassy carbons GC-10, 20, and 30 heat treated at 1000, 2000, and 3000°C. Densities of the composites are slightly lower than for the glassy carbons; in both cases they change little with HTT. Open porosities of the carbon composites are significantly higher than those in the glassy carbons; however, open porosities in the glassy carbons increase sharply with increasing HTT.

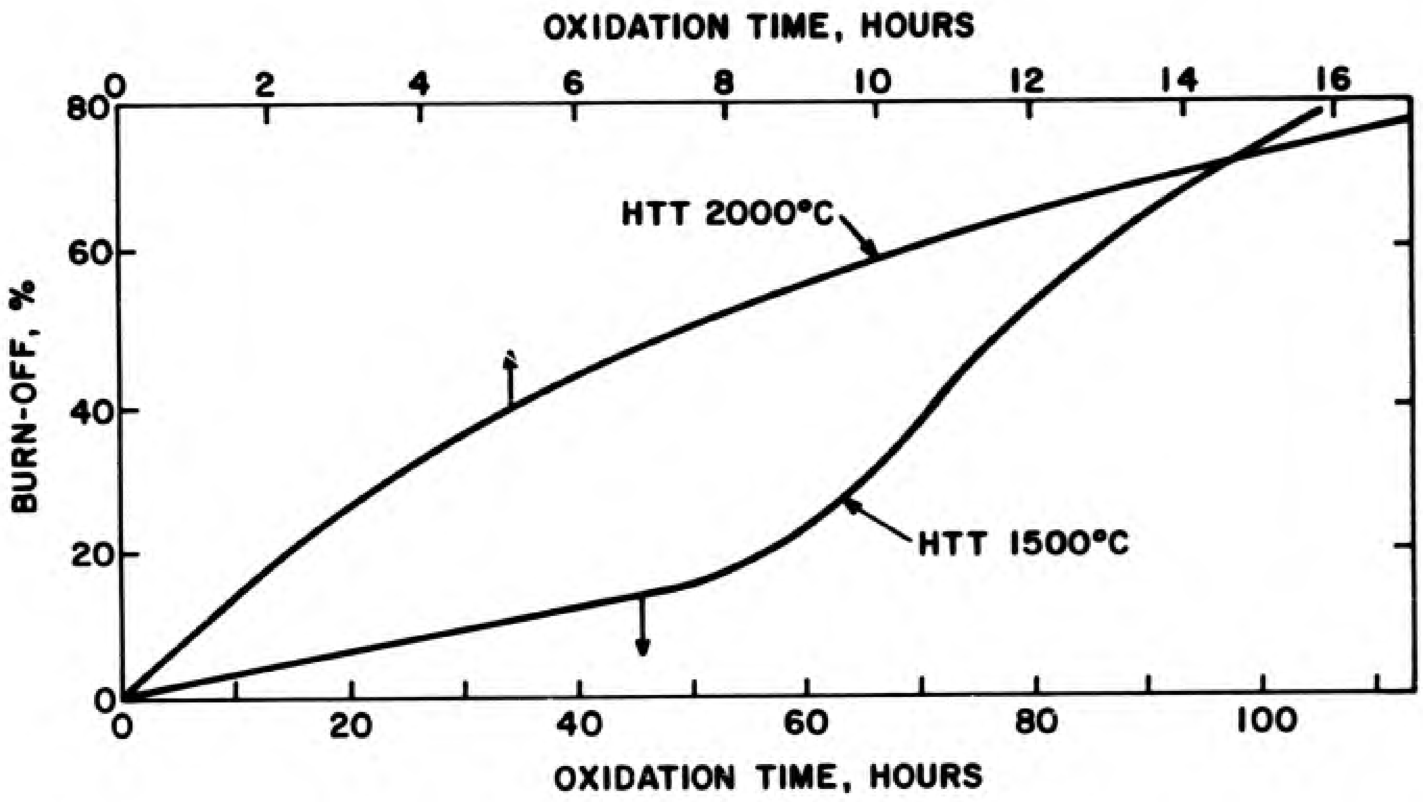

Fig. 10. Effect of heat treatment of composites at 1500°C and 2000°C on their reactivity in air at 500°C and 600°C, respectively.

TABLE 3

COMPARISON OF PROPERTIES FOR 72 HOUR INFILTRATED SAMPLES WITH THOSE OF TOKAI GLASSY CARBONS

Material	Apparent Density g/cc	Open Porosity %	Maximum Oxidation Rate, % Burn-off/hr	Flexural Strength kg/cm^2	Young's Modulus kg/mm^2	CTE[b] X10^6 $°C^{-1}$	Electrical Resistivity mohm·cm	Wear mg/500 Revol.	Hardness kg/mm^2
				Infiltrated Samples					
No HT	1.39	11.5	0.27[c]	820	2000	2.5	28	3.0	186
1000°C	1.43	13.9	0.13[c]	940	2150	2.1	10	4.7	205
1500°C	1.46	12.8	0.028[c]	1250	1950	1.4	7.2	8.7	173
2000°C	1.45	12.9	0.143[d]	1250	1800	1.4	7.2	65	128
2400°C	1.43	13.6	0.046[d]	1070	1550	1.4	7.1	190	110
				Tokai Samples[a]					
GC-10	1.48-1.51	0.2-0.4	(0.060)[c]	(830-935)	3000-3300	2.0-2.2	(11)	(1.4)	(273)
GC-20	1.47-1.50	1-3	(0.245)[d]	(925)	3000-3300	2.0-2.2	(8.3)	(1.5)	(234)
GC-30	1.44-1.47	3-5	(0.081)[d]	500-600	2200-2500	2.0-2.2	3.5-4.0	(10.5)	(154)

[a] Values were taken from reference (10); values in parentheses were determined by the authors

[b] For the interval 100-400°C (composites) or at 100°C (Tokai)

[c] Measured at 500°C

[d] Measured at 600°C

At comparable HTT, oxidation rates of the glassy carbons are higher than those for the carbon composites. For both materials oxidation rates decrease sharply with increasing HTT. In the case of the glassy carbons this may be due primarily to a decrease in ash content with increasing HTT. That is, in going from GC-10 to GC-30 the ash content is reported to drop from >1000 ppm to <100 ppm (10). At comparable HTT flexural strengths of the two carbons are similar, but Young's moduli of the glassy carbons are significantly higher. Whereas the CTE of the carbons for a HTT of 1000°C are comparable, the carbon composites have lower CTE values for treatment above 2000°C. For comparable HTT, electrical resistivities of the two carbons are similar. Wear resistance of both materials is seen to decrease with increasing HTT, but at comparable HTT the wear resistance of the glassy carbons is much superior to the carbon composites. The same situation holds for Knoop hardness values.

Glassy (and vitreous) carbons have found a number of metallurgical and mechanical applications as boats, crucibles, seals, and susceptors. It is interesting to speculate as to whether carbon composites as prepared in this study also have some applications in this field. It is expected that the total time required to produce the composites will be significantly less than that required to produce the glassy carbons because of the very long curing and carbonization cycle required in the latter case.

2.4 Conclusions

Cellulose powder can be compacted at room temperature into artifacts which upon curing and carbonization lead to bodies of low density (0.68 g/cc) and large open porosities (64%). In turn, the open porosity in these bodies can be filled by the deposit of carbon from the cracking of a hydrocarbon to produce a composite of higher density, increased strength and modulus, increased wear resistance and hardness, increased oxidation resistance, and decreased electrical resistivity The infiltration rate is governed by the open porosity by the equation $\theta_t = \theta_o \exp(-kt)$. A number of properties (Y) are related to the apparent density (d) of the artifact by the equation $Y = ad^b$ where values of a and b are functions of the particular property and HTT. Some properties of the composites produced using a long infiltration time (72 hr) are superior to those of commercial glassy carbons for comparable HTT (for example, oxidation resistance); whereas other properties are inferior (such as wear resistance).

2.5 References

1. Kotlensky, W. V., Chemistry and Physics of Carbon, (P. L. Walker, Jr. and P. A. Thrower, Editors), Vol. 9, Marcel Dekker, New York, 1973, p. 173.
2. Christner, L. G., Ph.D. Thesis, The Pennsylvania State University, 1972
3. Nagle, D. C. and Walker, P. L., Jr., Extended Abstracts, Eleventh Biennial Conference on Carbon, 1973, p. 322.
4. Dubinin, M. M., Chemistry and Physics of Carbon, (P. L. Walker, Jr., Editor), Vol. 2, Marcel Dekker, New York, 1966, p. 51.
5. Walker, P. L., Jr., Austin, L. G., and Nandi, S. P., ibid, p. 257.
6. Franklin, R. E., Acta Cryst., 3, 107 (1950).
7. Pinnick, H. T., Proceedings of the Conferences on Carbon, University of Buffalo, 1956, p. 3.
8. Laine, N. R., Vastola, F. J., and Walker, P. L., Jr., J. Phys. Chem., 67, 2030 (1963).
9. Walker, P. L., Jr., McKinstry, H. A., and Wright, C. C., Ind. Eng. Chem., 45, 1711 (1953).
10. Yamada, S., Report 68-2, Defense Ceramic Information Center, Battelle Memorial Institute, 1968.

3. NEW BINARY CARBIDE "GLASSES"

(S. A. Gallagher and R. Roy)

3.1 Introduction

One of the puzzles which faced V. M. Goldschmidt, the father of geochemistry and solid state chemistry, was his inability to make carbide glasses. The vast majority of inorganic glasses are based on an oxygen network, and many others based on the chalcogenides were already well-known in the mid-twenties to Goldschmidt. Some halide glasses were also known. Yet it was well known that no molten compounds with higher charged cations and anions e.g. nitrides and carbides (if indeed one can talk of N^{3-} and C^{4-} ions at all) could ever be cooled or quenched to a noncrystalline state. The reason normally accepted as the cause for the paradox that (even though the bond strengths are higher than in oxides) carbide glasses do not form has been that the melting points of carbides are so high that in such temperature regimes the KT is such that reorganization of the disordered noncrystalline phase into the stable crystal cannot be stopped.

In the late sixties Sarjeant and Roy (1) first expanded the range of noncrystallinity in oxide systems by utilizing splat and plasma spray techniques. More recently Messier and Roy (2) demonstrated that RF sputtering can expand even further the compositional range which can be retained in the non-crystalline state. It was the purpose of this paper to examine whether or not binary carbide glasses can be prepared by the same process.

3.2 Experimental

The sputtering was performed on an MRC model #8632 sputtering module. The samples were prepared by sputtering up from the target to the substrates. The target was a 2 inch diameter glassy carbon disc with either metal wires or a metal sheet of the various metals placed on the target in an off-center position. In the case of Dy, a metal powder was used. The substrates were 8x8 mm glass cover slides which were evenly spaced along the diameter of the target, perpendicular to the metal wires and sheets.

All tests were run using $3\text{x}10^{-2}$ torr Ar pressure and 28 mm target to substrate distance. Low powers of 25 and 50 watts were used to reduce the chance of crystallization of the metal. Fe and Dy were run at 100 watts to increase the deposition rate. X-ray diffraction, electron microprobe, electron microscope, resistivity measurements and heat treatment analysis were used to characterize the samples.

3.3 Results

The data show that binary glasses are formed in the carbon rich end of the system in every system studied. Furthermore, the studies show that there is a limit in the amount of metal which can be incorporated into the carbon matrix at which the particular metal will appear as a crystalline phase. Figure 1 shows this range of noncrystalline film formation for several metal-carbon systems. For some metals the limit of noncrystalline solid formation was not found. The limits of metal, determined in various systems thus far, is shown in Table 1. The noncrystallinity is established in each case by x-ray diffraction. Further, transmission electron diffraction patterns show only diffuse rings indicating a crystallite size of less than 25A. Such transmission electron micrographs (Figure 2) show fine grained homogeneous phases.

Heat treatments of the NCS prepared were performed at 150, 300, 450°C. All samples were x-rayed after heating for one hour in a resistance furnace with an argon atmosphere. All samples remained

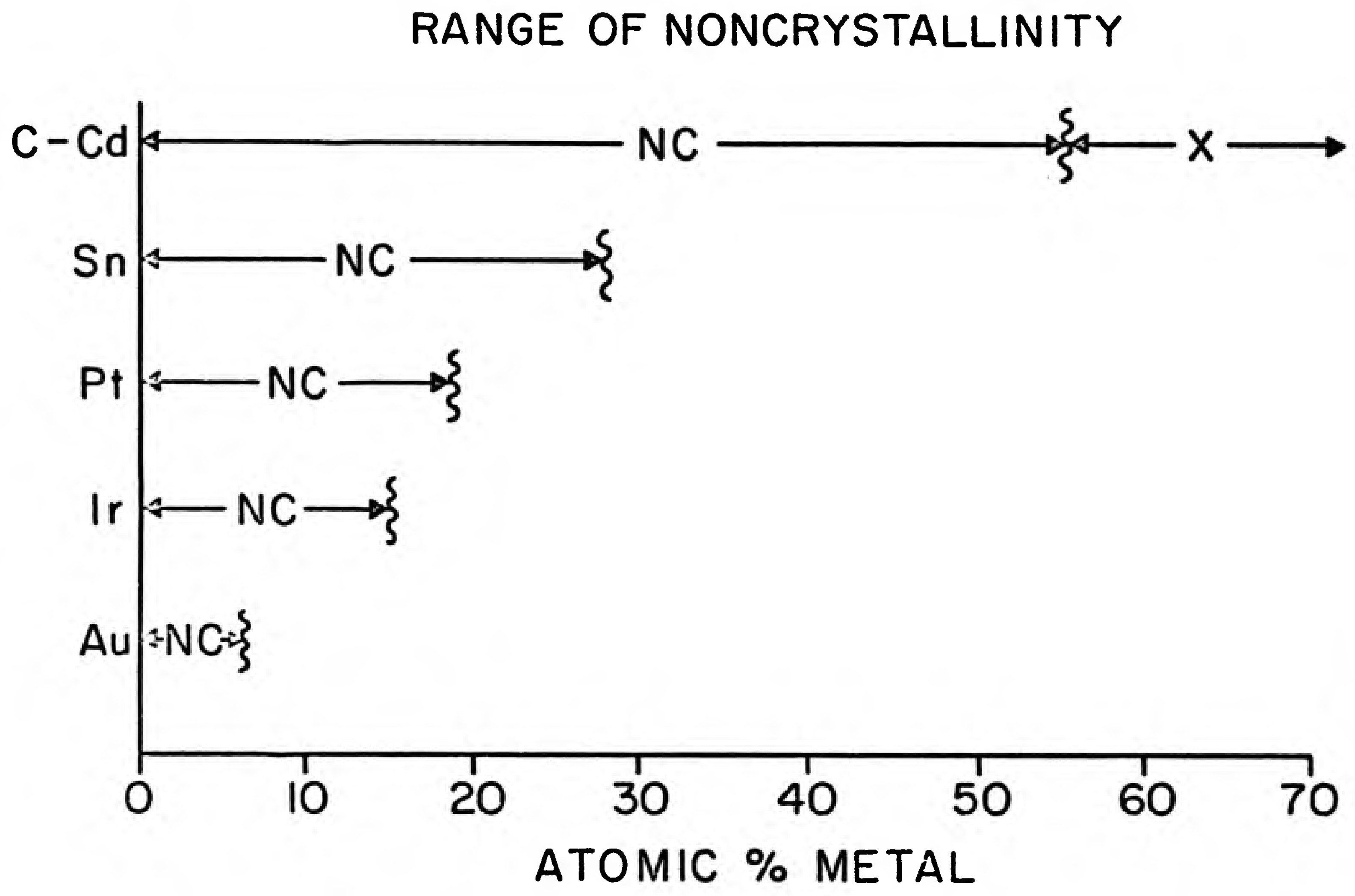

Fig. 1. Schematic illustration of the compositional extent of NCS prepared by RF sputtering in six metal-carbon systems.

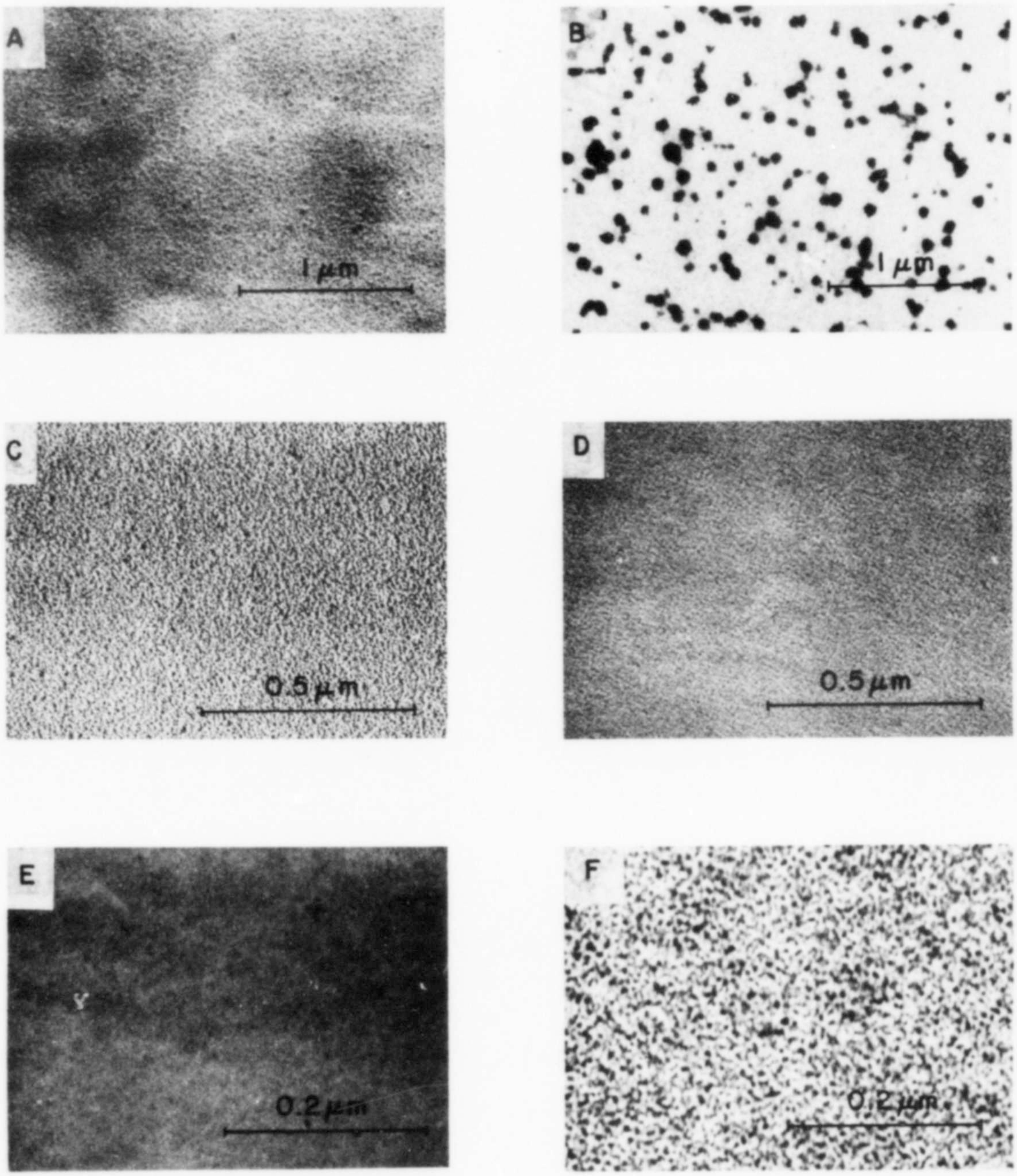

Fig. 2. Electron micrographs of (A) ∿4 at. % Fe-C; (B) ∿8 at. % Dy-C; (C) ∿10 at. % IR-C; (D) ∿12 at. % Pt-C; (E) ∿40 at. % Cd-C; and (F) ∿20 at. % Sn-C.

TABLE 1

PERCENTAGE METAL INCLUDED IN METAL-CARBON SAMPLES

Metal	Atomic %
Fe	30
Er	10
Dy	8
Cr	7
Al	6

noncrystalline to 450°C except the 30 atomic percent Fe-C film. This crystallized to form Fe, Fe_2O_3 and Fe_2O_4. Room temperature resistivity measurements were made using a two probe electrode configuration. The resistivities obtained are shown in Table 2. There is a range of six orders of magnitude difference in the resistivities for the same percentage of various metals.

TABLE 2

RESISTIVITIES OF METAL-CARBON SAMPLES

Metal	Resistivity, ohm-cm
Sn (25%)	3×10^{-3}
Pt (12%)	3×10^{-3}
Ir (10%)	3×10^{-3}
Au (6%)	1.5×10^{-1}
Fe (4%)	3×10^{-1}
Al (6%)	3×10^{3}
Er (10%)	1×10^{1}
Dy (8%)	8×10^{3}

3.4 References

1. P. T. Sarjeant and R. Roy, Reactivity of Solids, pp. 725-733, John Wiley and Sons, Inc. (1969).

2. R. Messier and R. Roy, Mat. Res. Bull., 6, 749 (1971).

4. PREPARATION AND PROPERTIES OF SPUTTERED "GLASSY" CARBON FILMS

(Z. Marinkovic and R. Roy)

4.1 Introduction

While an enormous literature exists on carbon films their systematic preparation by sputtering or ion-plating techniques has not been reported previously. The potential of marrying the desirable chemical properties of carbon to the technology of coatings is obvious. Moreover, there is some hope that by proper control one could prepare carbon films with a high proportion of tetrahedral bonding, i.e. with diamond-like structure and properties. Such hopes are based on the rather complete control we have learned to exercise on the process parameters in sputtering, which, for instance, made possible the preparation of sputtered films of noncrystalline Ge, with densities higher than diamond structure Ge.

The first attempts to prepare such sputtered carbon films in this laboratory gave mechanically stable films only when thicknesses were less than 7000A; thicker films peeled or buckled off the glass substrates (1). To investigate properties such as density and microhardness, one needs thicknesses of the order to 15-20μ. Thus the goal of this work was a systematic investigation of the optimum conditions for sputtering in order to obtain sufficiently thick carbon films, in order to study their structure and properties.

4.2 Experimental

The films were prepared using a Materials Research Corporation multi target sputtering system. Target diameters were 5 cm; the distance between target and substrate was kept at 30 mm. The pressure before sputtering was 3×10^{-6} torr. The carbon films were deposited on Corning cover glass substrates 8x8 mm and 18x18 mm, and on fused quartz 25x25 mm. Thickness of the films was measured after deposition using a Varian A-scope interferometer. Microstructure of the carbon films was evaluated using a JEOL JSM 50A Scanning Electron Microscope. Density was determined using the weight-geometry method. Knoop hardness was measured using a Leitz miniload hardness tester. Crystallinity of the sputtered carbon films was determined using a Picker-Siemens powder x-ray diffractometer (Ni-filtered copper Kα radiation). Composition of the sputtered carbon films was measured by electron microprobe analysis. Details of the sputtering conditions have been presented in earlier papers from this laboratory (2,3,4) and in previous reports.

In this work targets with three different structures were used: polycrystalline graphite, pyrolytic graphite and glassy carbon. With each target, 4 different Ar pressures (in the range 10-40 μm) were investigated and for each Ar pressure, the rf power was varied from 20W to 500W.

4.3 Results and Discussion

4.3.1 Influence of RF Power and Composition Rate

It was shown as expected, that the deposition rate from a graphite target increased rapidly with RF power (Figure 1) and attained values which made possible the preparation of 10-20 μm films. With increasing argon pressure, deposition rate increases as shown in Figure 2. Similar results were obtained for pyrolytic graphite and glassy carbon targets.

At 10 μm argon pressure, and with all the different levels of rf power used (i.e. from 20 watts to 500 watts), the glassy carbon films formed peeled during or after sputtering. With higher argon pressures, at all rf power levels used, no peeling occurs. At 20W, 50W and 100 W

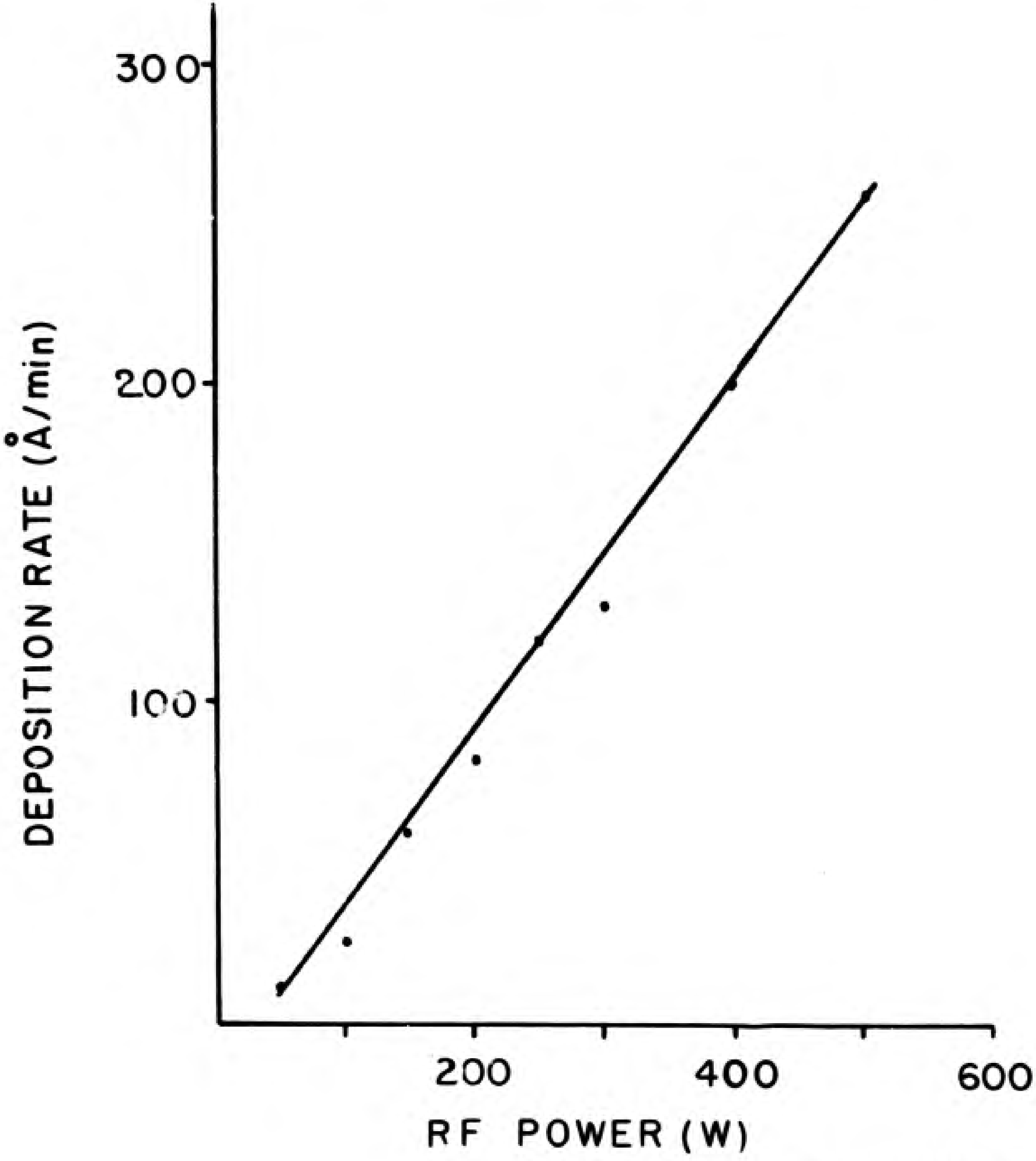

Fig. 1. Correlation of deposition rate with RF power.

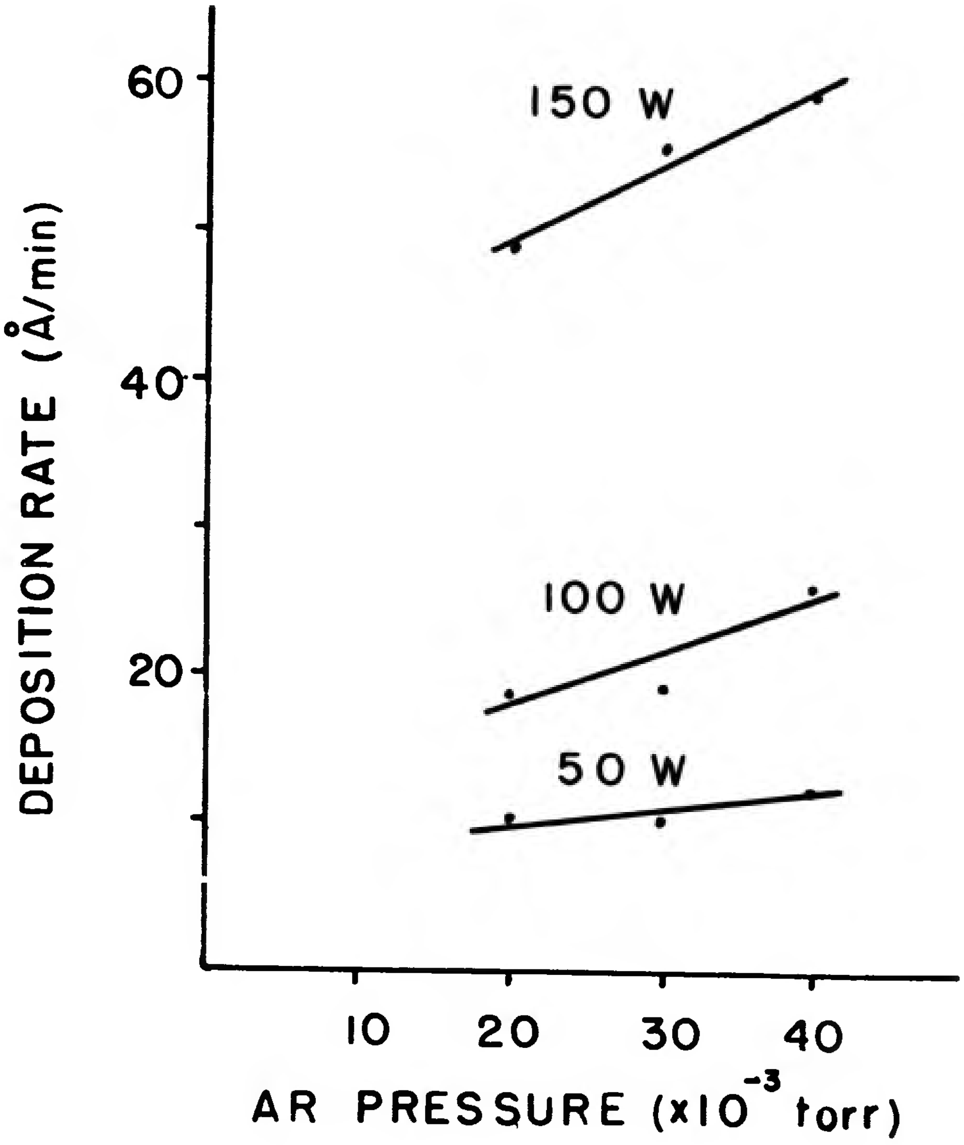

Fig. 2. Deposition rate of the graphite films versus Ar pressure for 3 different RF power.

rf power and with argon pressures of 30-40 μm, there is no peeling during the sputtering, but peeling occurs within a few days. In some of these films, peeling occurred after 1-2 months. However, both thin and very thick films, obtained at higher rf power, (200W, 300W, 400W, and 500W) are very stable and peeling does not occur at all.

Adhesion of the carbon films was checked using the 'scotch tape' test. The films obtained under all sputtering conditions on Corning cover glass slides have poor adhesion and can be stripped by means of the scotch tape. However, carbon films sputtered on fused quartz substrates, adhere very well, showing the influence of thermal expansion as, at least, one important parameter.

4.3.2 Structure and Microstructure

All carbon films sputtered from graphite, pyrolytic graphite and glassy carbon targets, onto both glass and fused quartz substrates are, as expected, noncrystalline, as verified by x-ray diffraction. Their microstructure, however, is very peculiar. They appear to have a 'pile of sand' structure, with grains in the 0.1-1.0 μm range. The porosity is evident even in the SEM photos. Figure 3 shows such microstructures of the 18 μm and 40 μm films obtained from a pyrolytic graphite target.

4.3.3 Densities

The most striking finding of the present work is the ability to prepare glassy carbon films with an enormous range of density, which depends almost entirely on rf power. With increasing rf power, the density of the sputtered carbon films decreases, probably as a consequence of increasing deposition rate and consequent entrapment of sputtering gases. The microhardness also decreases with increasing rf power, presumably due to decreasing density. Figure 4 shows the dependence of density and microhardness of sputtered films from a pyrolytic graphite

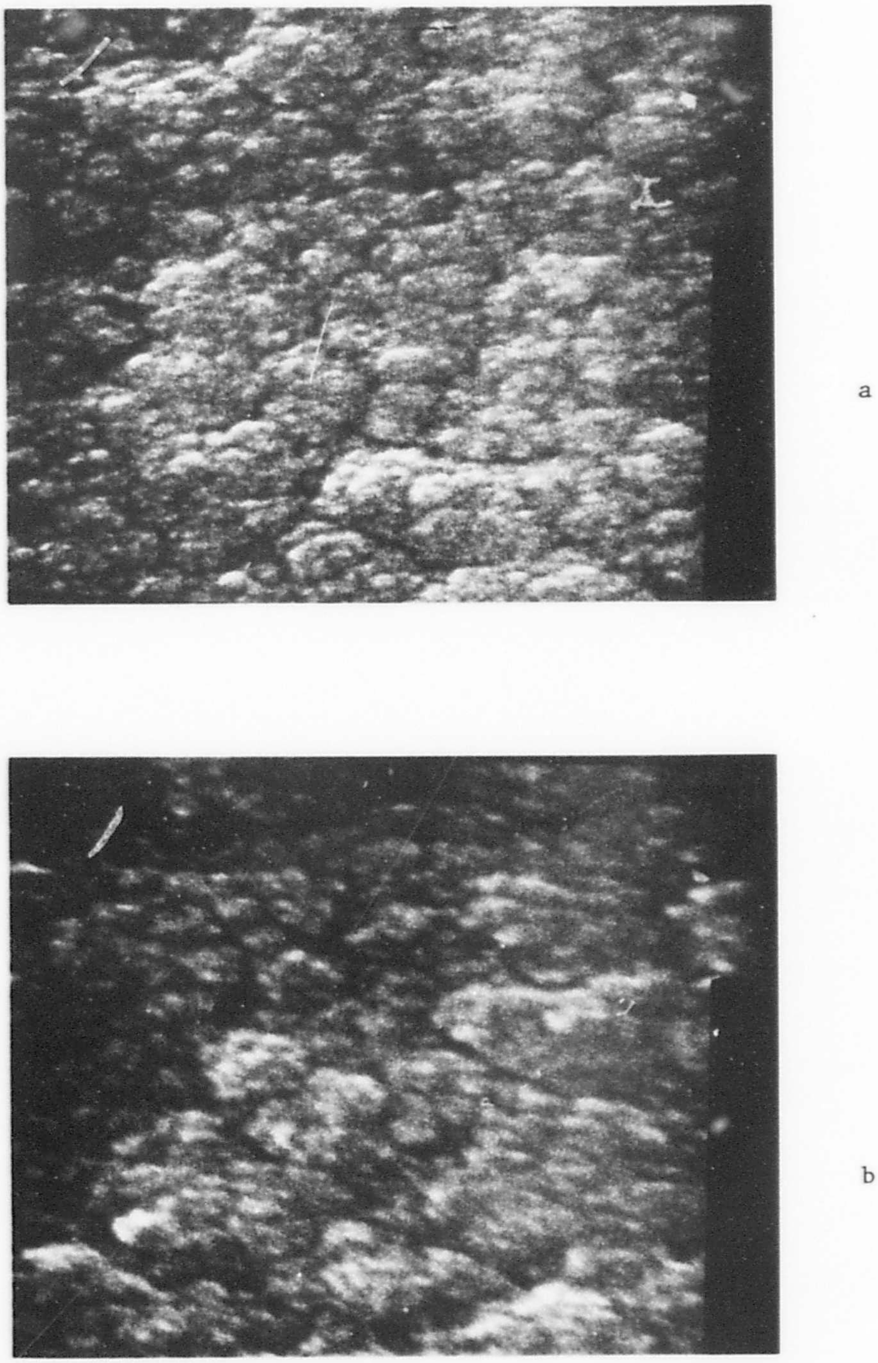

Fig. 3. SEM photograph of the pyrolytic graphite films thickness: a - 18μm; b - 40 μm.

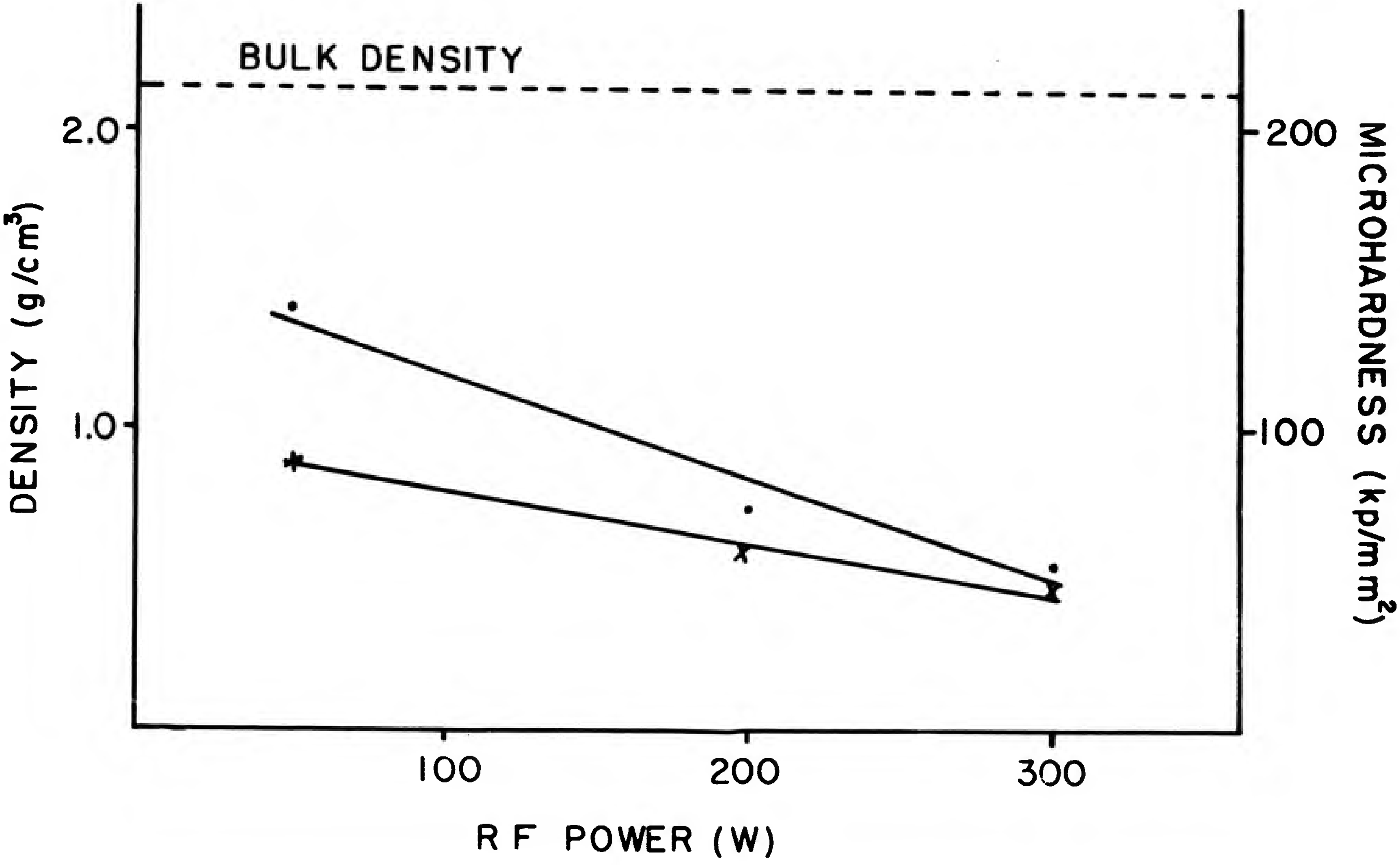

Fig. 4. Dependence of density (o) and hardness (x) of sputtered pyrolytic graphite films on RF power.

target on rf power. Similar results were obtained for films sputtered from a graphite target. Similar behavior has been noted by us for tellurium sputtered films, in which 'superdensity' films were obtained with the lowest rf power (20W)(5), and for Ge films (2).

4.3.4 Influence of Target

Densities of carbon films sputtered from three different targets, but under identical sputtering conditions (50W rf power; 30 μm argon pressure) are presented in Table 1.

TABLE 1

DENSITY OF SPUTTERED CARBON FILMS

Target Material	Density of the sputtered films (g/cm^3)	Bulk density of targets (g/cm^3)
Graphite	1.58	2.2
Pyrolytic graphite	1.40	2.15
Glassy carbon	0.74	1.5

It is very interesting for sputtering theory to note that the density of sputtered films depends dramatically on the target density. The density of all the "glassy" carbon films is lower than that of the corresponding targets. This, in itself is not unexpected for the graphite samples because the films are noncrystalline and most glassy carbons have $\rho = \sim 1.0\text{-}1.5$. However, it is surprising to find that the glassy carbon target with a nominal original ρ of 1.5 produced films with densities of only one-half that value (0.74). This conclusively proves that the species in the vapor is quite different and certainly quite high in molecular weight for the different target materials.

The control of density of the glassy carbon films was one of the main purposes of the work. Could we, in fact, produce glassy films with densities above the crystalline material, as we have already done in the case of Ge.

While our attempts to obtain such superdense carbon films did not produce the desired results, we obtained noncrystalline carbon films with the highest density yet reported (1.79 g/cm^3). This is obtained at the lowest power levels (20W) and at 30 μ argon pressure. From Figure 4 it is clear that in order to obtain denser films, the power should be further reduced. However, with lower power it is not possible to sustain the plasma.

A different approach was made to reach this objective by trying to sputter-up from a diamond target. This has proved to be impossible so far, since we can only utilize unconsolidated fine powder. This gets excessively heated in the plasma and tends to graphitize. We have been, so far, unable to either consolidate the diamond, without substantial adulteration or compact it into a "conducting" form.

It should also be noted that films sputtered from graphite and pyrolytic graphite targets with densities higher than 1.2 g/cm^3 and from the glassy carbon target with densities higher than 0.6 g/cm^3, are unstable towards peeling.

Another interesting observation was that the lower density film had open porosity whereas the denser materials had, at least some, closed porosity. Thus, the carbon, oxygen and argon contents in carbon films with different densities, were determined by electron microprobe and it was shown that low density carbon films do not contain measurable argon, but high density carbon films have up to 6 at. % of argon (Figure 5). (The increased argon content cannot account for increased density of these films). An oxygen content of about 2 at. % was found in all the investigated carbon films and probably corresponds to surface adsorption on these high surface area materials.

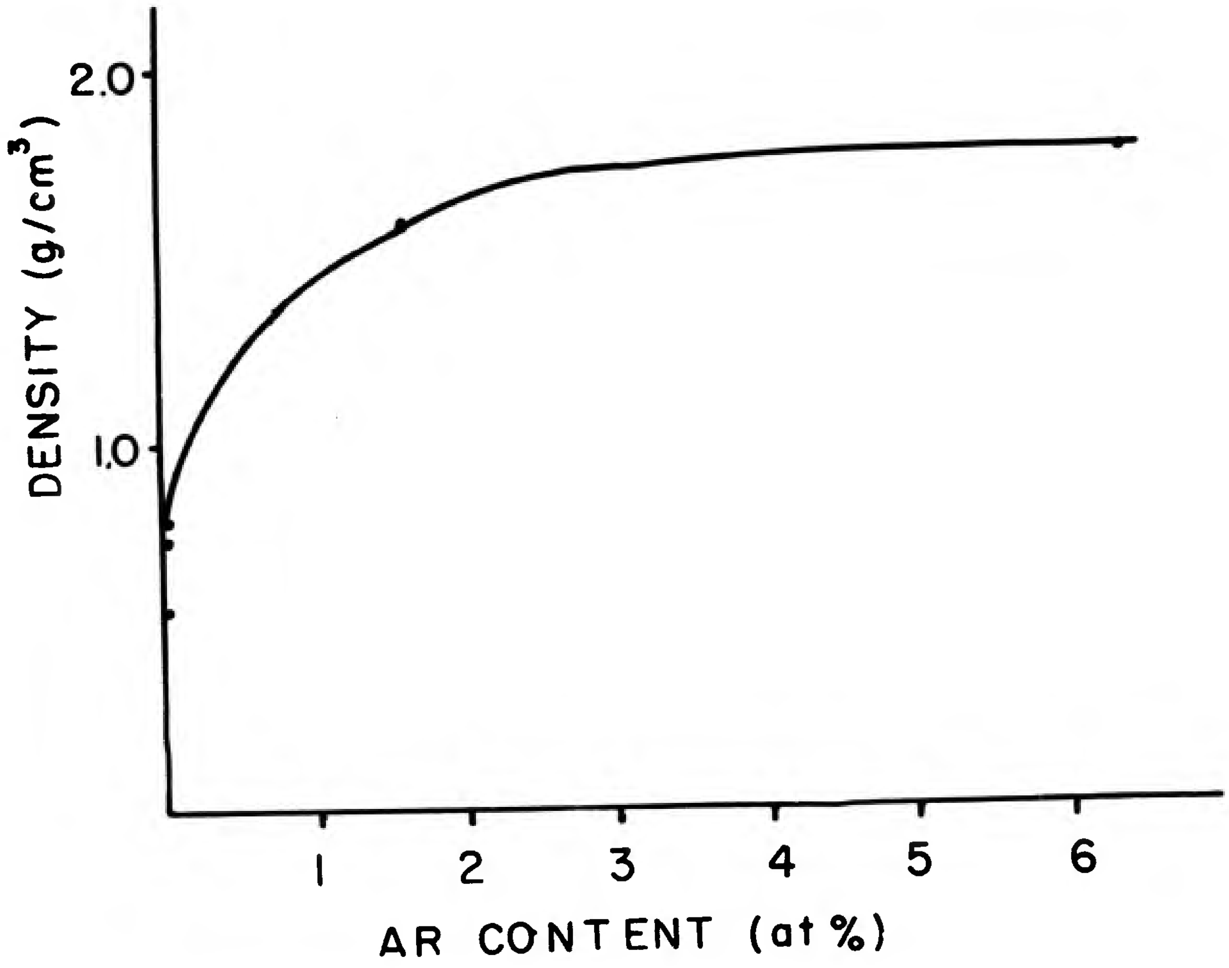

Fig. 5. Correlation of the density with argon content.

4.4 References

1. R. Roy and R. Messier, Glassy Carbon, Alloys, Semi-Annual Technical Report, January, 1973.

2. R. Messier, Ph.D. Thesis, The Pennsylvania State University, 1973.

3. R. Messier and R. Roy, Mat. Res. Bull., 6, 749 (1971).

4. R. Messier, A. K. Sarkar and R. Roy, Mat. Res. Bull., 9, 157 (1974).

5. Z. Marinkovic and R. Roy, (Thin Sol. Films, in press).